CONTROL OF THERMOGENESIS BY NUCLEAR RECEPTOR COREPRESSORS AND REV-ERBS IN BROWN ADIPOSE TISSUE

Hannah J. Richter

A DISSERTATION

in

Biochemistry and Molecular Biophysics

Presented to the Faculties of the University of Pennsylvania

in

Partial Fulfillment of the Requirements for the

Degree of Doctor of Philosophy

2022

Supervisor of Dissertation

Mitchell A. Lazar

Willard and Rhoda Ware Professor in Diabetes and Metabolic Diseases

Graduate Group Chairperson

Kim A. Sharp

Associate Professor of Biochemistry and Biophysics

Dissertation Committee

Kathryn E. Wellen (Chair), Professor of Cancer Biology

Patrick Seale, Professor of Cell and Developmental Biology

Paul M. Titchenell, Assistant Professor of Physiology

Nathaniel W. Snyder, Associate Professor of Cardiovascular Sciences, Temple University

CONTROL OF THERMOGENESIS BY NUCLEAR RECEPTOR COREPRESSORS AND REV-ERBS IN BROWN ADIPOSE TISSUE

Dedicated to the mice that gave their lives for scientific progress

ACKNOWLEDGMENT

First and foremost, I must thank my parents, Andi and Erich Richter. They have always been my most important support mechanism and my strongest cheerleaders. No matter what I have chosen to do with my life, they have always encouraged me to do the best at it. They keep me entertained with book recommendations, stories of our cats, television show updates, and plenty of board games when we can find the time. Graduate school has not been an easy experience, but I know it would have been impossible without my parents just a phone call away.

Second, I need to express my love for my “family” in Philadelphia: my partner Omar Navarro Leija and my cat Clara. Both make sure I leave the lab sometimes and get enough sleep and food to keep me healthy and happy. Without them, this degree would not have been finished and I want them to know that I will always love them. I am so excited to move our little family in together (with Llamita, of course!) and start the next adventure in life.

Thank you to Matt Emmett, who first trained me in the lab and has forever influenced the way I do and think about science. I hope we always keep in touch and can chat about science or swimming or life in general at any time.

Thank you to all members of the Lazar lab, past and present but especially Sean Armour, Jarrett Remsberg, Dave Steger, Lindsey Peed, Marine Adlanmerini, Amy Hauck, Pieterjan Dierickx, Yehuda Shabtai, Brianna Krusen, Bryce Carpenter, Delaine Zayas-Bazan, Lauren Woodie, and Michael Tackenberg. You’ve all contributed to my success in your own way, and I couldn’t have done it without you.

Thank you to my mentees, Corey Holman and Bethany Nahri So. You both pushed me to know my own science well enough to teach it and then taught me so much in return. I hope we remain friends and colleagues for many years to come.

Thank you to the Biochemistry and Molecular Biophysics Graduate Group and especially my cohort. We did it! With lots of drinks, talks, and fun along the way. A special thanks to Kelli McKenna, Kim Sharp, and Kristen Lynch for being fearless leaders of a growing and changing group of rambunctious scientists.

Thank you to all my mentors during my undergraduate years, both in science and outside of science. You impacted my thinking deeply and helped me pursue whatever path interested me the most. Namely, Matt Tedesco, Phil Shields, Kevin Braun, Dina Simkim, and Ileana Soto.

And finally, thank you to Mitch Lazar, who has been with me over six years as I learned what it means to be a scientist and how to push science forward. Your training will always be with me as I move through the next stages of my life.

ABSTRACT

CONTROL OF THERMOGENESIS BY NUCLEAR RECEPTOR COREPRESSORS AND REV-ERBS IN BROWN ADIPOSE TISSUE

Hannah J. Richter

Mitchell A. Lazar

Brown adipose tissue (BAT) is a key thermogenic organ, whose expression of Uncoupling Protein 1 (UCP1) and ability to maintain body temperature in response to acute cold exposure requires histone deacetylase 3 (HDAC3). HDAC3 exists in tight association with nuclear receptor corepressors NCoR1 and NCoR2 (also known as Silencing Mediator of Retinoid and Thyroid Receptors, or SMRT), but the functions of NCoR1/2 in BAT have not been established. This corepressor complex of HDAC3 and NCoR1/2 can interact with a variety of nuclear receptors, including REV-ERBα/β which are related nuclear receptors (NRs) that couple the molecular clock with metabolism. Here we report that, as expected, genetic loss of NCoR1/2 in BAT (NCoR1/2 BAT-dKO) leads to loss of HDAC3 activity. In addition, HDAC3 is no longer bound at its physiological genomic sites in the absence of NCoR1/2, leading to a shared deregulation of BAT lipid metabolism between the NCoR1/2 BAT-dKO and HDAC3 BAT KO mice. Despite these commonalities, however, loss of NCoR1/2 in BAT does not phenocopy the cold sensitivity observed in the HDAC3 BAT-KO, nor does loss of either corepressor alone. Instead, BAT lacking NCoR1/2 is inflamed, particularly with respect to the IL-17 axis that increases thermogenic capacity by enhancing innervation. Integration of BAT RNA-seq and ChIP-seq data revealed that NCoR1/2 directly regulate *Mmp9*, which integrates extracellular matrix remodeling and inflammation. We also find that REV-ERBα/β do not tissue-autonomously control acute

and circadian BAT thermogenesis. However, BAT REV-ERBα/β do regulate lipogenesis via Srebp1c in conditions of chronic cold. These findings reveal pleiotropic functions of the NCoR/HDAC3 corepressor complex in BAT, and one of their associated nuclear receptor partners, REV-ERBα/β. In sum, HDAC3-independent suppression of BAT inflammation counterbalances NCoR1/2 stimulation of HDAC3 activity in the control of thermogenesis, while REV-ERBα/β only control thermogenesis in BAT via fuel availability.

TABLE OF CONTENTS

LIST OF TABLES

LIST OF ILLUSTRATIONS

CHAPTER 1: Background

Obesity and brown adipose tissue

As the medical world begins to cope with the effects of COVID-19 on our collective physical and psychological well-being, we return to thinking about other health crises. One such health crisis, that is also a risk factor for COVID-19 complications, is the obesity epidemic (Albashir 2020). Obesity rates continue to rise, with limited therapeutic options available (Y. Wang et al. 2020; Ruban et al. 2019). The current primary therapies are difficult lifestyle changes or invasive surgeries, leading many pharmaceutical companies to search for a pharmacological method for weight loss, though these are often plagued by undesirable or dangerous side effects (Dragano et al. 2020). Therefore, new pharmacological targets are needed to broaden the possible avenues for effective and safe weight loss.

The weight of any organism can be considered a balance between input and output of biomass, or for animals, the balance between calories consumed and energy expended. While there are many factors, both physical and social, influencing the weight of any individual human, weight loss or gain can only be achieved by disrupting the balance of this scale, the mechanisms of which are described in **Figure 1.1**. It is important to note that unhealthy weight can occur on both the higher and lower bounds and anorexia and obesity are sometimes considered two diseases of the same spectrum (Tsai et al. 2016). In fact, both types of disordered eating increased in prevalence during the initial COVID-19 pandemic (Sideli et al. 2021). However, here we will focus on obesity as the therapeutic avenue being discussed is one that increases energy expenditure, which is undesirable for anorexic patients.

Adipose tissue is the primary organ responsible for storage of energy in the form of lipids. Weight gain predominantly occurs via expansion of the white adipose tissue (WAT) and this expansion can occur in a multitude of mechanisms that impact the overall health of the tissue and the organism (K. Sun, Kusminski, and Scherer 2011; Meister et al. 2022; Vishvanath and Gupta 2019). There is another type of adipose tissue which also stores carbon for energy in lipid droplets but whose primary function is not storage. This is the brown adipose tissue (BAT), which is the focus of this dissertation. BAT is a thermogenic organ, as in, it produces heat (Cannon and Nedergaard 2004). There is also beige or brite adipose, which is inducible and located within white adipose depots and will not be discussed here in detail (W. Wang and Seale 2016). Brown adipose is a distinct organ from white adipose, both in location and in function.

Historically, brown adipose was first commonly identified in biology texts as “the hibernating gland”, found in small mammals such as hedgehogs and rats; these sources cite works from as early as 1670 (Rasmussen 1923; Sheldon 1924). In the 1960s this tissue was determined to be important for the thermogenic requirements of newborn human infants, though it’s role in adult humans was still debated (Aherne and Hull 1966; Brück 1961; Lidell 2019). Further study of this tissue in the 1970s revealed two key features that are still important today: the presence of a 32 kilodalton (kDa) protein in the mitochondria and norepinephrine-stimulated oxygen consumption (Ricquier and Kader 1976; Heaton et al. 1978; Nedergaard, Cannon, and Lindberg 1977; Nedergaard and Lindberg 1979). It was not until much more recently that brown adipose tissue (BAT) was identified and found to be functional in adult humans, sparking a renewed interest in this unique thermogenic organ (Cypess et al. 2009; van Marken Lichtenbelt et al. 2009).

But why is BAT of particular interest when considering treatments for obesity or metabolic disease? The answer lies in that 32kDa protein first identified in the 1970s: that protein is UCP1 or uncoupling protein 1. This is a fascinating inner mitochondrial membrane protein found only in brown or beige adipose and canonically responsible for those organs' ability to produce heat. One function of UCP1 is to dissipate the proton gradient that is normally used to produce ATP, and this dissipation converts chemical energy to heat (Nicholls and Locke 1984). Activation of BAT can consume large amounts of fuel in order to continue producing that proton gradient via the tricarboxylic acid cycle (TCA cycle) and the electron transport chain (ETC). In fact, activation of BAT in human subjects can increase resting metabolic rate (RMR) by over 200 kcal per day in some accounts (Cypess et al. 2015). Therefore, much work has been applied to figuring out how to activate brown adipose safely and effectively, which requires a strong background knowledge in how the tissue is normally activated. To understand canonical pathways of activation, researchers turned to the classic mouse model, as mice have active interscapular brown adipose tissue and (unlike humans) can easily be bred to contain various genetic changes that may affect thermogenesis.

I have summarized the classical activation pathway of BAT in **Figure 1.2**, leaving out many details and auxiliary mechanisms, based on several key reviews of this field (Cannon and Nedergaard 2004; Bolsoni-Lopes, Deshaies, and Festuccia 2015; Tabuchi and Sul 2021). This key pathway goes as follows: cold exposure causes the sympathetic nervous system to release norepinephrine (NE), NE activates the β_3 adrenergic receptors which are highly present in BAT, this activates the classic cAMP and PKA kinase cascade, this cascade both activates lipolysis and has transcriptional effects via p38, p38 activates PGC-1α which serves as co-activator for many transcription factors including PPARγ

ATF2, and ERRs, upregulating expression of *Ucp1* and metabolic pathways including OXPHOS. Meanwhile, lipolysis both provides fuel to the TCA cycle and the ETC while generating free fatty acids (FFAs) which are required for activation of UCP1 activity. In sum, this pathway leads to a host of short and long-term metabolic changes, depending on the length of the stimulus and allows the tissue to efficiently generate heat. This heat is then dissipated to the organism via the blood, as BAT is highly vascularized (Mrzilkova et al. 2020).

While this pathway may initially appear to offer many avenues of therapeutic input, much of this pathway overlaps with pathways key for cardiac and muscle metabolism, meaning side effects can be highly problematic. Therefore, it continues to be important to fully understand the mechanisms by which BAT is activated to find targets unique to thermogenesis. An area that has gained traction in recent years is UCP1-independent mechanisms of thermogenesis. This initially began with the observation that UCP1 knockout (KO) mice, which lack UCP1 in all tissues at all times, can still be acclimated to cold conditions, albeit they are sensitive to acute cold (Ukropec et al. 2006). Since then, several alternative pathways have been identified to provide heat in brown or beige adipose, which have been thoroughly reviewed elsewhere and will not be discussed further here (Roesler and Kazak 2020; Chouchani, Kazak, and Spiegelman 2019). Those alternative pathways still occur in the adipocytes themselves, but an area of new interest to the field is the contribution of other cell types, particularly immune cells, to thermogenesis in brown or beige adipose.

Immune cells, especially macrophages and T cells, have been previously of interest to the obesity field due to their functions in maintaining the health of white adipose tissue (WAT) and changes in inflammation with expansion of WAT depots (Schäffler and

Schölmerich 2010; Lumeng and Saltiel 2011). TNF-α has been implicated as a key cytokine pathway for communication between white adipocytes and immune cell types (Cawthorn and Sethi 2008; C. P. Vieira et al. 2020). But for thermogenic adipose, the story has been more complicated. Initially macrophages were reported to synthesize catecholamines and thereby directly contribute to thermogenesis in beige adipose, but this was controversial and later disproven (Nguyen et al. 2011; Fischer et al. 2017). Recently, IL-17 signaling has gained traction as a contributor to the biology of both beige and brown adipose (Greenhill 2021; Hu et al. 2020; Pestel et al. 2020; Teijeiro et al. 2021). While immunology and metabolism are both complex fields on their own with many questions to be answered, it is also important to consider the regulation of these processes at a basic level: transcription.

Nuclear receptors and corepressors

Transcriptional regulation can include a host of regulatory levels from RNA polymerase pausing to chromatin compaction to looping of enhancers and promoters. The section of transcriptional regulation I will focus on here is that of nuclear receptors and their coregulators. Nuclear receptors were initially defined by their ability to directly integrate external signals with transcription by virtue of containing both a ligand binding domain and a DNA binding domain (Weikum, Liu, and Ortlund 2018). While nuclear receptors were first identified in the 1970s, nuclear receptor biology has since expanded as a field and encompasses physiology and pathology from adipogenesis to hormonal cancers (Evans and Mangelsdorf 2014). Nuclear receptors often bind to DNA as heterodimers that are structurally affected by ligand binding, as is typified in the first crystal structure of nuclear receptors on DNA, of PPARγ and RXRα (Chandra et al. 2008). The binding sites for such heterodimers and homodimers are palindromic or direct repeats of

AGGTCA or AGGACA spaced by a varying number of nucleotides (Weikum, Liu, and Ortlund 2018).

Additionally, nuclear receptors interact closely with a suite of coactivators and corepressors that can modulate their activity accordingly. Note that in the structure of PPARγ and RXRα cited above, they included and crystalized separate peptides containing an LXXLL motif, which is conserved among coactivators (Heery et al. 1997). There are also conserved motifs for corepressors termed the CoRNR box that are (L/I)XX(I/V)I or LXXX(I/L)XXX(I/L) (Nagy et al. 1999). Coactivators and coregulators have direct competition for binding to nuclear receptors and this binding is mediated through the flexible helix 12 (also known as the activation function helix) which changes conformation with ligand binding (Nagy et al. 1999; Weikum, Liu, and Ortlund 2018). This switch from availability for corepressor binding with no ligand and availability for coactivator binding with ligand is known as a coregulator switch and helps amplify and ligand-dependent signal; see **Figure 1.3A** for a diagrammatic explanation of this switch (Nagy and Schwabe 2004). While this is the classical model for nuclear receptor gene regulation, more nuanced and complex models exist with varying degrees of evidence, including but not limited to squelching, coactivator redistribution, a coregulator shift, and various ideas of indirect DNA binding known as tethering (Schmidt et al. 2016; Shabtai et al. 2021; Zhang et al. 2015).

Here we will focus on the classical coregulator switch, or more specially, a singular corepressor complex that can interact with various nuclear receptors and therefore respond to a multitude of ligands and cell signaling pathways. That corepressor complex is that which contains HDAC3, NCoR1 or NCoR2, as well as a host of accessory proteins. NCoR1 and NCoR2 (SMRT) were in fact the first corepressors in which the CoRNR box

was described (Nagy et al. 1999). NCoR1/2 are large, highly homologous, approximately 270 kDa proteins, which can be thought of as the core of this complex and are exchangeable such that a typical complex contains either NCoR1 or NCoR2 (Privalsky 2004). Deletion of either NCoR1 or SMRT is embryonic lethal, indicating that, despite their similarities, they are not redundant (Jepsen et al. 2000; 2007).

Previous work has shown NCoR1 and SMRT to be important for several metabolism-related processes, though less is known regarding SMRT. Liver-specific deletion of NCoR1 results in hepatic steatosis (Z. Sun et al. 2013), while adipocyte-specific deletion reportedly leads to insulin sensitivity (Li et al. 2011), macrophage deletion yields an anti-inflammatory phenotype (Li et al. 2013), and muscle deletion results in increased muscle mass and endurance (Yamamoto et al. 2011). For this proposal it is worth noting the adipose-specific deletion was utilizing *Ap2*-Cre which has since been shown to be expressed in multiple tissues including brain, liver, and muscle (Mullican et al. 2013; Jeffery et al. 2014). Mice lacking one SMRT allele gain increased weight on high-fat diet (Sutanto et al. 2010), while mice with mutations in the receptor interacting domains exhibit increased weight as well as reduced respiration and respiratory distress syndrome at birth (Pei et al. 2011; Nofsinger et al. 2008; Reilly et al. 2010). Most recently, epidermal stratification is NCoR1/2 -dependent (Szigety et al. 2020), and inducible deletion of NCoR1 and NCoR2 leads to death of an adult mouse with notable lipodystrophy and hypoglycemia (Ritter et al. 2021).

But let us return to the other key member of this corepressor complex, HDAC3. One may be wondering what exactly the mechanism is by which a nuclear receptor and its auxiliary proteins are able to affect gene expression. The mechanism at play here is histone acetylation. To understand fully how histone acetylation and transcription are

related, it is necessary to take a brief detour to explain chromatin biology. The basic repeating unit of chromatin is the histone octamer wrapped with 146 base pairs of DNA, known as a nucleosome. This poses a structural problem for RNA polymerase. Much work has gone into understanding how RNA polymerase is able to handle this issue of DNA being wrapped around histones, and this continues to be an area of structural and biochemical study (Kujirai and Kurumizaka 2020). While this process undoubtedly involves a host of complexes, particularly various chromatin remodelers that have the ability to use ATP to slide DNA along histones or even evict subunits of the octamer (Reyes, Marcum, and He 2021), here I want to focus back on this issue of acetylation.

Histones each have an extended N-terminal domain colloquially known as the tail, which can be decorated with a variety of functional post-translational modifications in a combinatorial fashion often called the “histone code” (Strahl and Allis 2000). Each of these modifications have readers, writers, and erasers which interpret, add, or remove these marks respectively. HDAC3 is a well-studied histone deacetylase, as in it removes acetylation from histone tails. The mechanism of HDAC-mediated deacetylation includes a catalytic zinc ion coordinating a nucleophilic attack which results in the acetyl-lysine being released as acetate and L-lysine, which in HDAC3 specifically requires the active site residue Y298 (Lombardi et al. 2011; Sun et al. 2013). The result of this acetyl removal is broad, but generally leads to compaction of chromatin and reduced accessibility to the DNA for RNA polymerase and other transcription factors to the DNA in that area (Tolsma and Hansen 2019). HDAC3 deacetylase function also requires interaction with the aptly-named deacetylase activating domain of either NCoR1 or NCoR2, with this interaction coordinated by IP_4, as seen in the crystal structure shown in **Figure 1.3B** (Guenther, Barak, and Lazar 2001; Watson et al. 2012; You et al. 2013). HDAC3 also has a variety

of tissue-specific function as described above for NCoR1/2 that have been recently reviewed (Emmett and Lazar 2019). Together, the NCoR1/2 and HDAC3 complex interact with nuclear receptors to actively repress gene expression by histone deacetylation in a manner with requires all members of the complex.

We previously published a surprisingly role for HDAC3 in the activation of *Ucp1* expression through the coactivator PGC-1α (Emmett et al. 2017). My work in **Chapter 2** sought to determine the contributions of NCoR1/2 to this mechanism and uncovered a further surprising function for NCoR1/2 in HDAC3-independent regulation of inflammation.

Circadian rhythms and metabolism

Biological clocks synchronize many processes with the daily cycle of light and dark. While first discovered in plants, these genetically encoded clocks are now known to be present in mammals and driven by a central clock located in the suprachiasmatic nuclei (Takahashi et al. 2008; Bass 2012). Peripheral clocks, such as those in adipose, potentially play a significant role in disease and metabolism (Allada and Bass 2021; Guan and Lazar 2021). The interrelationship of circadian and metabolic systems is complicated by the fact that many tissues and cell types contribute to the metabolic state. It has been suggested that adipose tissues have an important function in coordination of whole-body energy balance in a circadian manner and dysregulation of adipose clocks can contribute to metabolic disorder (Henriksson and Lamia 2015; E. Vieira et al. 2014).

The core molecular clock is present in nearly every cell in the body and maintains an endogenous approximately 24-hour rhythm that can be entrained by signals such as light and feeding. This core transcriptional loop is as follows: a heterodimer of transcription factors CLOCK and BMAL1 drive transcription of CRY and PER proteins which heterodimerize and subsequently repress CLOCK:BMAL1, but CRY and PER undergo

ubiquitin-mediated degradation in a timed manner so that the cycle can begin again (Partch, Green, and Takahashi 2014). There is a second loop in which RORα drives the expression of BMAL1 while REV-ERB binds at the same site to repress the expression of BMAL1; see the left of **Figure 1.4** (Guan and Lazar 2021). REV-ERB is a nuclear receptor that uniquely mediates the connection between the molecular clock and metabolism in tissue-specific manners that are summarized in the right panel of **Figure 1.4**. However, some of these studies, particularly the function of REV-ERBα in thermogenesis were done using a whole-body KO model (Gerhart-Hines et al. 2013). **Chapter 3** covers my efforts to determine whether this effect is tissue-specific to the BAT and what exactly REV-ERBs are controlling in BAT metabolism.

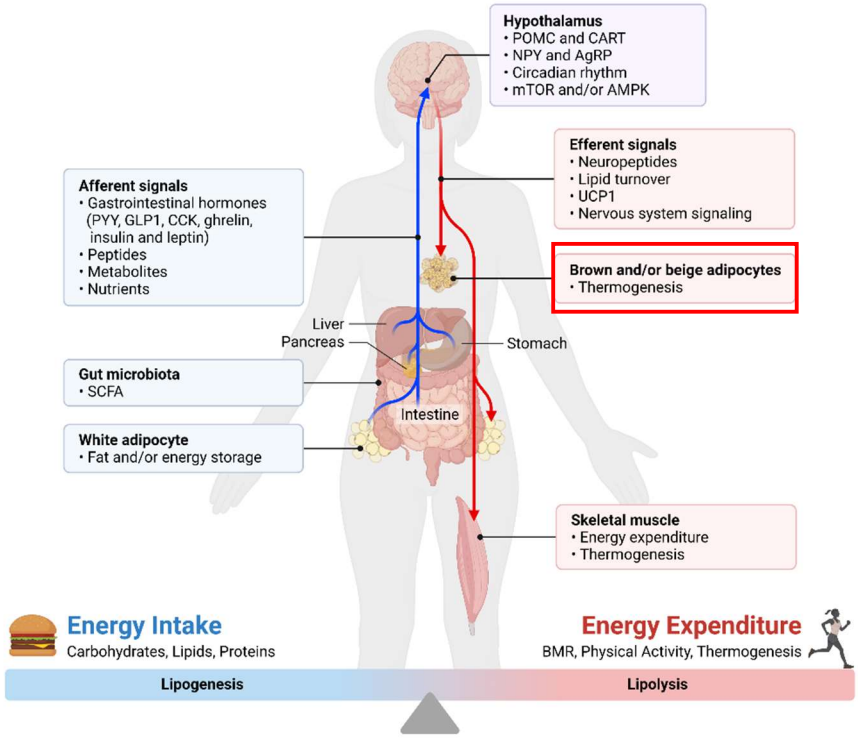

Figure 1.1. Key mechanisms contributing to body weight. An overview of the multitude of mechanisms in different organs that can contribute to overall body weight. Thermogenesis highlighted in red square. Reprinted from “Key Metabolic Mechanisms on Body Weight Regulation”, by BioRender.com (2022). Retrieved from https://app.biorender.com/biorender-templates.

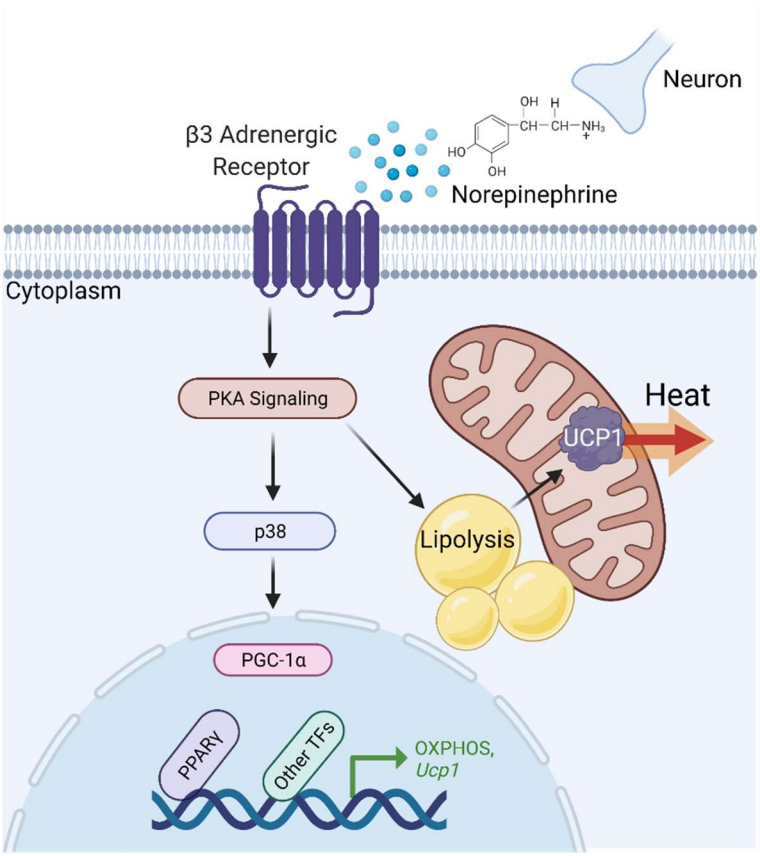

Figure 1.2. Classical thermogenic signaling in brown adipocytes. Begins with norepinephrine (NE) release from neurons, activating the B3 adrenergic signaling via PKA which stimulates lipolysis and p38. Lipolysis stimulates UCP1-dependent heat generation through free-fatty acids (FFAs) and acetyl-CoA as fuel for the electron transport chain. p38 also stimulates PGC-1a which can coactivate a variety of transcription factors and nuclear receptors, inducing transcription of *Ucp1* and OXPHOS genes. PKA: Protein Kinase A. PGC-1a: peroxisome proliferator-activated receptor gamma coactivator 1-alpha. PPARg: peroxisome proliferator-activated receptor gamma. Other TFs (transcription factors): include ATF2, ERRs, TRs, etc. OXPHOS: oxidative phosphorylation. UCP1: uncoupling protein 1. Adapted from “GPCR Molecular Pathway (Layout)”, by BioRender.com (2022).

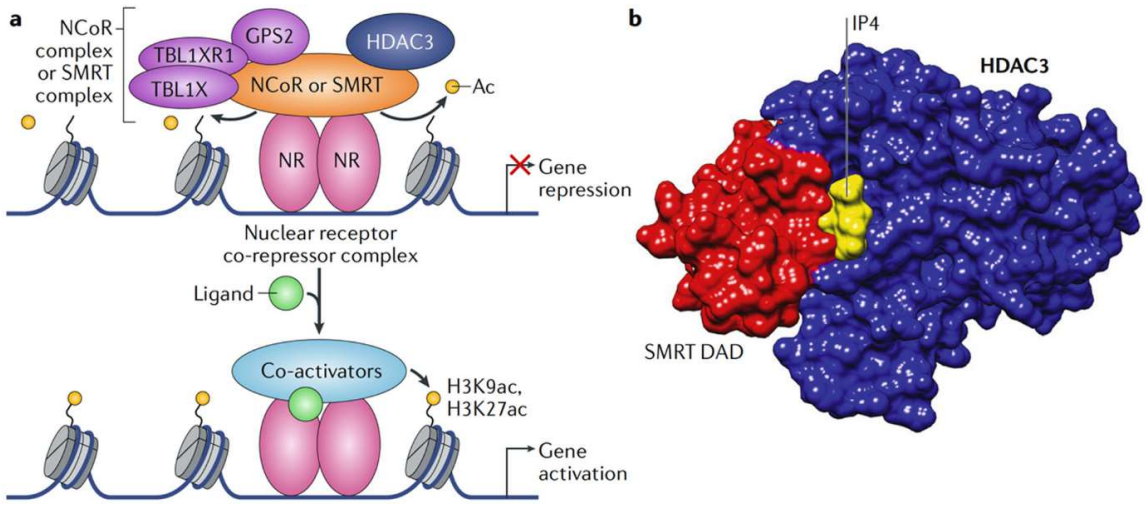

Figure 1.3. **Nuclear receptor transcriptional activity is modulated by an HDAC3-containing corepressor complex. A.** Corepressor/coactivator switch regulates transcription via acetylation of histone 3. **B.** Crystal structure of coordination of the DAD domain of SMRT with HDAC3, an interaction required for histone deacetylase activity. Ac: acetyl group, GPS2: G protein pathway suppressor 2, H3K27ac: acetylated histone H3 lysine 27, H3K9ac: acetylated histone H3 lysine 9, NCoR: nuclear receptor co-repressor 1, SMRT: Silencing Mediator Of Retinoic Acid and Thyroid Hormone aka NCoR2, NR: nuclear receptor, TBL1X: transducin b-Like 1 X-Linked, TBL1XR1, TBL1-reLated protein 1, DAD: deacetylase-activating domain, IP4: inositol phosphate 1,4,5,6. From Figure 1 of "Integrative regulation of physiology by histone deacetylase 3" (Emmett and Lazar 2019). **B** crystal structure image taken by Hannah J. Richter.

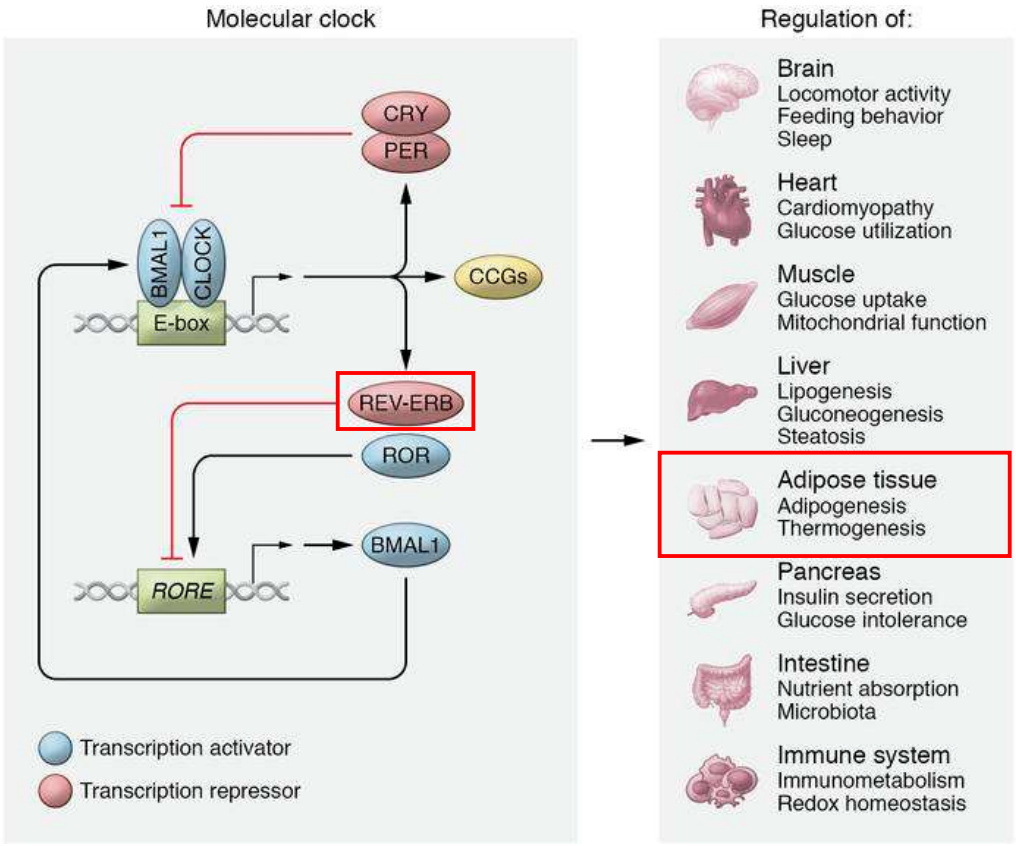

Figure 1.4. Regulation of metabolic tissues by the molecular clock. The molecular clock, shown on the left, is made of a loop of transcriptional activators and repressors that are primarily known to regulate core clock genes (CCGs). The molecular clock can also regulate metabolism in a variety of tissue-specific mechanisms, as shown on the right. REV-ERB and adipose tissue highlighted in red squares. CRY: Cryptochrome Circadian Regulator, PER: Period Circadian Regulator, BMAL1: (transcript is *Arntl*) Aryl Hydrocarbon Receptor Nuclear Translocator Like, CLOCK: Clock Circadian Regulator, ROR: RAR Related Orphan Receptor, RORE: ROR response element. From Figure 1 of "Interconnections between circadian clocks and metabolism" (Guan and Lazar 2021).

CHAPTER 2: Balanced Control of Thermogenesis by Nuclear Receptor Corepressors in Brown Adipose Tissue

This article has been accepted for publication as:

Richter, Hannah J., Hauck, Amy K., Batmanov, Kirill, Inoue, Shin-Ichi, So, Bethany N., Kim, Mindy, Emmett, Matthew J., Cohen, Ronald N., and Mitchell A. Lazar. "Balanced control of thermogenesis by nuclear receptor corepressors in brown adipose tissue" *Proceedings of the National Academy of Sciences*, In Press. July 2022.

Hannah J. Richter designed and performed majority of experiments, performed statistical analysis and RNA-sequencing analysis, made all figures, and wrote the manuscript.

Abstract

Brown adipose tissue (BAT) is a key thermogenic organ, whose expression of Uncoupling Protein 1 (UCP1) and ability to maintain body temperature in response to acute cold exposure requires histone deacetylase 3 (HDAC3). HDAC3 exists in tight association with nuclear receptor corepressors NCoR1 and NCoR2 (also known as Silencing Mediator of Retinoid and Thyroid Receptors, or SMRT), but the functions of NCoR1/2 in BAT have not been established. Here we report that, as expected, genetic loss of NCoR1/2 in BAT (NCoR1/2 BAT-dKO) leads to loss of HDAC3 activity. In addition, HDAC3 is no longer bound at its physiological genomic sites in the absence of NCoR1/2, leading to a shared deregulation of BAT lipid metabolism between the NCoR1/2 BAT-dKO and HDAC3 BAT KO mice. Despite these commonalities, loss of NCoR1/2 in BAT does not phenocopy the cold sensitivity observed in the HDAC3 BAT-KO, nor does loss of either corepressor alone. Instead, BAT lacking NCoR1/2 is inflamed, particularly with respect to the IL-17

axis that increases thermogenic capacity by enhancing innervation. Integration of BAT RNA-seq and ChIP-seq data revealed that NCoR1/2 directly regulate *Mmp9*, which integrates extracellular matrix remodeling and inflammation. These findings reveal pleiotropic functions of the NCoR/HDAC3 corepressor complex in BAT, such that HDAC3-independent suppression of BAT inflammation counterbalances stimulation of HDAC3 activity in the control of thermogenesis.

Introduction

Obesity is an ongoing metabolic health crisis that lacks simple and effective therapeutics (1, 2). One potential avenue for the treatment of obesity is the activation of calorie consumption by brown adipose tissue (BAT) (3, 4). BAT is a major thermogenic organ in mammals and known to be active in adult humans, especially in response to adrenergic cold stimulus (5, 6). BAT uses fuels such as glucose and lipids to produce heat via uncoupling protein 1 (UCP1), a mitochondrial membrane protein which releases the mitochondrial proton gradient independent of ATP production (7). UCP1-independent thermogenic mechanisms are also possible, coming from sources such as creatine and calcium metabolism (8). A less well-studied contribution to thermogenesis is inflammation of BAT itself (9).

Inflammation of white adipose is implicated in obesity and related metabolic disease pathogenesis, with specific macrophage subpopulations and crown-like structures often associated with poor adipose health (10–12). For beige adipose, macrophages and inflammation are commonly linked to a reduction in thermogenic capacity with obesity, though mechanisms of macrophage-adipose communication are debated (13–16). More recently, $\gamma\delta$T cells have been shown to positively effect BAT

thermogenesis through cytokines IL-17A and IL-17F (17, 18). However, the transcriptional underpinnings of this novel thermogenic pathway have yet to be uncovered.

Nuclear receptors regulate gene expression by recruitment of specific coactivator or corepressor complexes to affect nearby histone post-translational modifications (PTMs) (19). These coregulators are targets of interest for a variety of diseases (20). One such corepressor complex is the NCoR-HDAC3 complex, of which histone deacetylase 3 (HDAC3) is the enzymatic component (21). Nuclear receptor corepressor 1 (NCoR1) or NCoR2 (also known as SMRT) are required to activate the deacetylase function of HDAC3 (22). Previous work has described the requirement of HDAC3 for acute thermogenic capacity in BAT, in part by deacetylating and activating Peroxisome Proliferator-Activated Receptor Gamma Coactivator 1-Alpha (PGC1-α) which is a coactivator for thermogenic Estrogen Related Receptor Alpha (ERRα) (23).

Since the canonical deacetylase function of HDAC3 requires interaction with NCoR1/2, we hypothesized that depletion of NCoR1/2 in BAT would phenocopy the cold intolerance of mice lacking HDAC3 in BAT. Surprisingly, we found that, unlike HDAC3, NCoR1/2 were not required for the acute thermogenic stimulation of BAT even though HDAC3 genomic binding and activity were dramatically attenuated. In-depth analysis of BAT genes specifically dysregulated in the absence of NCoR1/2 but not HDAC3 revealed the induction of inflammatory pathways, especially IL-17 signaling which promotes thermogenic innervation of the tissue. Thus, NCoR1/2 regulate inflammation and thermogenesis through mechanisms distinct from HDAC3 in BAT.

Results

The canonical repressive role of HDAC3 in BAT requires NCoR1/2.

To study tissue-specific functions of the nuclear receptor corepressors NCoR1 and NCoR2, floxed alleles for both corepressors were crossed with mice transgenic for *Ucp1*-Cre on a C57BL/6J background to knock out (KO) NCoR1/2 in brown adipocytes (24, 25). These alleles allow efficient depletion of BAT NCoR1/2 protein in the single KOs (sKOs) (**Fig. S1A**). The levels of NCoR1 and 2 mRNA (**Fig. 1A**) were markedly depleted in BAT from the double KO mice (hereafter referred to as NCoR1/2 BAT-dKO mice) with minimal effect on the expression of other key components of the complex, such as histone deacetylase 3 (HDAC3) and G Protein Pathway Suppressor 2 (GPS2) (**Fig. 1A**). Of note, whereas NCoR1 protein was also diminished in the NCoR1/2 BAT-dKO, levels of NCoR2 were similar to those in control mice (**Fig S1B**). The floxed alleles were deleted as expected (**Fig. S1C**), and thus we suspect that the residual protein is in a non-brown adipocyte cell type specific to the dKO. For example, NCoR2 expression is highly enriched in macrophages (26) and, as shown below, the dKO BAT is characterized by increased immune cells. Additionally, the enzyme activity of HDAC3 immunoprecipitated from NCoR1/2 BAT-dKO BAT lysates was reduced to an extent indistinguishable from that of HDAC3 in BAT lacking HDAC3 in brown adipocytes (**Fig. 1B**), with remaining activity likely coming from non-adipocytes in the tissue.

We next performed HDAC3 chromatin immunoprecipitation followed by sequencing (ChIP-seq) in BAT from Control, NCoR1/2 BAT-dKO, and HDAC3 BAT-KO animals. This analysis led to the identification of 6406 high-confidence HDAC3 sites as defined by Control signal at least 4-fold greater than in the HDAC3 BAT-KO (**Fig. S1D**). 85% of these peaks were lost in the NCoR1/2 BAT-dKO (**Fig. S1D**) and HDAC3 binding was highly reduced overall (**Fig. 1C**). Motif analysis of control peaks with lost HDAC3 binding in the NCoR1/2 BAT-dKO these peaks (**Fig. 1D**) showed high enrichment for transcription factors known to be important for brown adipose lineage including EBF,

C/EBP, and Peroxisome Proliferator-Activated Receptors (PPARs) (27). Motif analysis of the HDAC3 peaks remaining in the NCoR1/2 BAT-dKO and new HDAC3 binding in the NCoR1/2 BAT-dKO revealed enrichment for ETS factors, including SpiB (**Fig. 1E**). These peaks were overall considerably weaker than the HDAC3 peaks in control BAT (**Fig. S1E**), and likely emanated from HDAC3 that remained in non-adipocytic cells including immune cells in which ETS factors play important roles (28, 29). HDAC3 peaks that were present only in control BAT were near genes enriched for brown adipose and related lineages (**Fig. S1F**) while HDAC3 peaks found in NCoR1/2 BAT-dKO are near genes enriched for lung and immune-related cell types (**Fig. S1G**). Additionally, 491 HDAC3 peaks in NCoR1/2 BAT-dKO tissue overlapped with those in macrophages (30), with high enrichment for the ETS motif of immune cell factor SpiB (**Fig. S1H**), whereas only 71 peaks overlapped between HDAC3 in control BAT and macrophages (**Fig. S1I**). These data are consistent with a model in which the residual and gained HDAC3 peaks in the dKO tissue are primarily occurring in non-adipocyte cell types in which NCoR1/2 were not deleted.

We next compared the transcriptomes of BAT lacking HDAC3 (23) with that of BAT lacking NCoR1/2 from animals housed at thermoneutrality for two weeks to remove thermogenic inputs. Using cut-offs of $p<0.05$ and $FC>1.5$, 778 unique transcripts were found to be co-regulated by HDAC3 and NCoR1/2 (**Fig. 1F**). The upregulated transcripts were enriched for PPARγ related lipid handling pathways (**Fig. 1G**), consistent with the role of NCoR1/2-HDAC3 complex as a coregulator of PPARγ in adipose tissue as well as the enrichment of the PPARγ binding motif at sites bound by NCoR1/2 and HDAC3 (31, 32). These findings were validated by RT-qPCR for transcripts encoding key lipid metabolism genes (**Fig. S1J**). The shared downregulated transcripts were not significantly

enriched for specific pathways. Together these data show that NCoR1/2 are required for physiological genomic location and deacetylase function of HDAC3 in BAT, which together regulate lipid metabolism.

Corepressor KO models do not phenocopy the cold intolerance observed in HDAC3 BAT-KO

Given that NCoR1/2 are required for BAT HDAC3 function at the genome, we next sought to determine if their loss would result in impairment of heat production as the loss of HDAC3 does in BAT. In agreement with previous studies (23), loss of HDAC3 resulted in marked impairment of norepinephrine-induced thermogenesis, as measured by oxygen consumption in a continuous lab animal monitoring system (CLAMS) (**Fig. 2A**). Surprisingly, however, NCoR1/2 BAT-dKO animals displayed no discernable change in thermogenic oxygen consumption compared to control mice (**Fig. 2B**). These animals also did not display any basal changes in metabolic parameters over 72 hours of monitoring (**Fig. S2**). We also tested individual loss of NCoR1 or NCoR2 in BAT to determine whether one but not the other was responsible for the HDAC3 thermogenic phenotype. BAT NCoR1-sKO mice actually displayed improved thermogenic output (**Fig. 2C**), potentially related to its partnership with circadian nuclear receptor REV-ERBα, which is a negative regulator of BAT thermogenesis (33). However, simultaneous loss of NCoR1 and HDAC3 phenocopied the HDAC3 BAT, indicating that the role of HDAC3 was dominant over that of NCoR1 (**Fig. 2D**). Deletion of NCoR2 in BAT had no appreciable effect on thermogenesis (**Fig. 2E**), and the impaired thermogenesis of HDAC3 KO BAT was retained when NCoR2 was also depleted (**Fig. 2F**). animals. Thus, thermogenesis was impaired by loss of HDAC3 in BAT, and this was not phenocopied by the loss of NCoR1/2, alone or together.

Loss of BAT NCoR1/2 induces thermogenic inflammation

The finding that NCoR1/2 depletion in BAT led to a reduction in HDAC3 enzyme activity and genomic functions but did not phenocopy the physiological effects of HDAC3 loss suggested that additional functions of NCoR1/2 might somehow compensate or balance the effects of HDAC3 inactivation on thermogenesis. To address this, we focused on the over 2000 genes that were differentially expressed in the NCoR1/2 dKO BAT but not HDAC3 KO BAT (**Fig. S3A**). 1145 transcripts were upregulated, matching the canonical repressive function of NCoR1/2, and gene ontology analysis revealed that this set of genes was highly enriched for immune-related pathways (**Fig. 3A**). Genes related to IL-17 signaling were uniquely enriched in BAT lacking NCoR1/2 (**Fig. 3B**), which was of particular interest since IL-17 signaling via γδT cells has been shown to promote thermogenesis (17, 18) and thus had the potential to offset the thermogenic defect associated with loss of BAT HDAC3.

We next isolated the stromal vascular fraction of the BAT, which excludes adipocytes and is enriched for immune cells, among other cell types (34). This analysis confirmed that NCoR1/2 were not depleted in the non-adipocytic cells of BAT in the KO models (**Fig. 3C**)**.** Moreover, as predicted from the bulk transcriptomics of the BAT, γδT cell genes such as *Ccl2* and *Il17f* were upregulated in these non-adipocytic cells, as were other γδT cell-related genes including *Cd4* and *Il17a* whose regulation did not reach significance in bulk transcriptome (**Fig. 3C**). Consistent with this, an increase in immune cells in the NCoR/1/2 BAT dKO was observed by immunohistochemistry (IHC) for CD45, a pan-hematopoietic marker, and CD68, a monocyte lineage marker (**Fig. 3D**). By

contrast, these inflammatory markers were essentially unchanged in HDAC3-sKO BAT (**Fig. S3B**).

IL-17 signaling has been reported to enhance thermogenesis by increasing the sympathetic innervation of BAT, which activates the tissue (17, 35, 36). Immunofluorescence (IF) staining for neuronal markers tyrosine hydroxylase (TH) and Tubulin Beta 3 Class III (Tubb3) revealed a robust increase in the NCoR1/2 BAT-dKO (**Fig. 3E-F**), but not in HDAC3 sKO BAT (**Fig. S3C-D**). Together these data demonstrate that the unique consequence of NCoR1/2 loss in BAT to induce the IL-17 inflammatory axis with an associated increase in thermogenic innervation, which is known to increase thermogenic output.

NcoR1/2 directly repress Mmp9, a key immune signaling factor

Since the increases in immune cells and IL-17 gene expression were likely indirect effects of the specific depletion of NCoR1/2 in brown adipocytes, we next sought to determine the direct transcriptional targets of NCoR1/2 that led to this phenotypic outcome. 525 genes that were transcriptionally upregulated in NCoR1/2 BAT-dKO, but not NCoR sKO or HDAC3 KO transcriptomes, had a nearby binding peak for NCoR1 in BAT (23) (**Fig. 4A**). These peaks were enriched for NFIL3, NF1, and SpiB binding motifs (**Fig. S4A**) and did not overlap with control HDAC3 peaks (**Fig. S4B**). Analysis of these putative direct NCoR target genes showed that cellular components involved in the extracellular matrix (ECM) were highly enriched (**Fig. 4B**) as was Tumor Necrosis Factor (TNF) signaling (**Fig. 4C**). By contrast, induction of numerous ECM genes in NCoR1/2 BAT-dKO was not observed in the BAT KO of HDAC3, nor of NCoR1 or 2 alone (**Fig. 4C**). ECM remodeling, particularly via matrix metalloproteases (Mmps), is known to cause immune cell infiltration into solid tissues and tumors (37). Indeed, *Mmp9* was markedly induced in

the NCOR1/2 KO BAT (highlighted, **Fig. 4D and 4E**). *Mmp9* showed a notable and specific internal NCoR1 binding peak, with little HDAC3 present at the same site (**Fig. 4F**). We also confirmed *Mmp9* upregulation in the NCoR1/2 BAT-dKO and not in the HDAC3 BAT-KO by RT-qPCR in a separate cohort, alongside confirmation of other key transcripts (**Fig. S4C**). Thus, the direct effect of NCoR1/2 deletion in brown adipocytes leading to pro-inflammatory signals was a putative cause of the secondary immune infiltration and IL-17 activation in the BAT lacking NCoR1/2.

To further confirm the effect of NCoR1/2 deletion on *Mmp9*, primary pre-adipocytes were harvested from BAT of *Rosa26-CreER* NCoR1/2 floxed animals and control floxed animals. This system displayed good KO efficiency and confirmed direct upregulation of *Mmp9* in brown adipocytes with loss of NCoR1/2 (**Fig. 4G**). Importantly, the loss of NCoR1/2 did not alter adipocytic differentiation as reflected by gene expression (**Fig. S4D**) or lipid accumulation (**Fig. S4E**). Together these data suggest that loss of NCoR1/2 in adipocytes directly induced *Mmp9* and potentially other pro-inflammatory signals that, in NCoR1/2 BAT-dKO mice, promoted the accumulation and activation of Th17 cells and resulted in increased thermogenic inflammation.

Discussion

Non-shivering thermogenesis is a physiological response to cold that is mediated in part by BAT, with many regulatory mechanisms and inputs to maintain temperature homeostasis and adaptability (5, 38). Here we have described a new role for NCoR1/2 in BAT in repressing pro-thermogenic inflammation via IL-17. This balances the well-established role of NCoR1/2 as obligate activators of the activity of HDAC3 (22, 39), which functions in BAT as a pilot light required for activation of the coactivator PGC1α and UCP1 (23) (**Fig. 5**).

HDAC3, NCoR1, and NCoR2 share the canonical function of repression of sets to genes to which NCoR1/2 get recruited by nuclear receptors and other sequence-specific transcription factors (39). The present findings that NCoR1/2 are required for HDAC3 activity and genomic localization are consistent with these principles, particularly at sites bound by BAT lineage factors including PPARs near genes involved in lipid metabolism (29, 31, 40). However, additional levels of complexity have emerged, including functions of HDAC3 that do not require its enzyme activity (41) as well as mechanisms by which HDAC3 may function as a transcriptional coactivator on specific genes (23, 30).

In macrophages, NCoR1/2 are known inflammatory regulators and there are sets of genes to which HDAC3 is recruited without NCoR1/2 (30, 42). Here we describe functions of NCoR1/2 in brown adipocytes that are distinct from the functions of HDAC3 in these cells. This is perhaps not surprising since NCoR1/2 are the largest components of a multiprotein repressor complex that also includes TBL1/TBL1R and GPS2 in stoichiometric proportions (37, 43–45). NCoR1/2 bind independently to TBL1/1R (43, 46), and the phenotypes of mice with tissue-specific loss of these components differ in severity and mechanism (47–51), consistent with each component nucleated by NCoR1/2 having separable and sometimes opposing functions. Loss of NCoR1/2 would be expected to result in phenotypes that combine the effects of loss of all of the components, and potentially additional NCoR1/2-specific outcomes. Our finding that loss of NCoR1/2, but not HDAC3, in brown adipocytes leads to inflammation of BAT defines one such NCoR1/2-specific function.

The inflammatory response in NCoR1/2 BAT-dKO involves an increase in IL-17 signaling associated with $\gamma\delta$T cells. This pathway has recently been shown to increase thermogenesis (17, 18), which could balance the reduction in thermogenesis due to loss of HDAC3 (**Fig. 5**). Different studies have implicated either IL-17A or IL-17F, and indeed,

we observe an increase in both γδ T cell cytokines in the NCoR1/2 depleted BAT (17, 18). One mechanism by which IL-17 signaling enhances thermogenesis is by increased innervation of BAT (17), which we observed in the NCoR1/2 BAT KO.

In this model, NCoR1/2 are deleted in brown adipocytes but not in other cellular components of BAT. As such, the increase in IL-17 signaling is likely an indirect effect of changes in the brown adipocyte. Transcriptomic analysis of the tissue as well as in primary brown adipocytes lacking NCoR1/2 has implicated upregulation of matrix metalloproteases, which are known to lead to inflammation in cancer (52, 53) as well as in white adipose tissue (54–58). Mmp9, which is increased in obese patients with insulin resistance and sensitive to pioglitazone treatment (59), is markedly induced in BAT lacking NCoR1/2 but not HDAC3. Other factors are also likely to contribute to the immune infiltration observed in the NCoR1/2 dKO BAT. In addition, the exact mechanism by which NCoR1/2 represses *Mmp* and other ECM-related genes, and how this signals to resident inflammatory cells remains to be determined.

Materials and methods

Animal Husbandry

All animal studies were performed under protocols approved by the University of Pennsylvania Perelman School of Medicine Institutional Animal Care and Use Committee (IACUC). Mice were group-housed in a temperature- and humidity-controlled, specific-pathogen–free animal facility at 22°C under a 12:12-h light–dark cycle with free access to standard chow (LabDiet, 5010 post-weaning; breeding on LabDiet 5021) and water. Mice were moved to an incubator set to 30°C two weeks (14 days) prior to sacrifice or phenotyping unless otherwise noted, with all tissue collection done at ZT10.

Floxed models, NCoR1$^{loxP/loxP}$ mice (Jackson Labs, strain: 033452)(24), NCoR2 (SMRT)$^{loxP/loxP}$ (60), and HDAC3$^{loxP/loxP}$ (Jackson Labs, strain: 024119) (61) mice were bred to heterozygous *Ucp1*-Cre expressing mice (Jackson Labs, strain: 024670) and maintained on a C57BL/6J background. All BAT-dKO animals were generated by crossing sKO animals in-house. All experiments were carried out on 11- to 14-wk-old male littermates generated from *Ucp1*-Cre heterozygous males mated to floxed allele homozygous females, weaned into shared housing.

Isolation and Quantification of RNA (RT-qPCR)

RNA was isolated from snap-frozen BAT as previously described (23) using TRIzol-chloroform extraction followed by RNeasy Mini spin columns (Qiagen) and on-column DNase-digestion

(Qiagen). RNA from cell culture was isolated using the RNeasy Mini kit protocol (Qiagen). Between 1-2μg of total RNA was reverse transcribed to cDNA using a HighCapacity cDNA Reverse Transcription kit (Applied Biosystems). RT-qPCR was performed using standard curve-based normalization and Power SYBR Green PCR Master mix on the Quant Studio 6 Flex Real-Time PCR system (Applied Biosystems), with all transcripts further normalized to *18s* quantity and average expression in the control group. Biological replicates shown in bar graphs. See primer table (**Table S1**) for specific primer sequences.

Histone Deacetylase 3 Activity

HDAC3 activity was assayed using the HDAC3 activity assay kit (Sigma Aldrich EPI004). Protein lysates were quantified by BCA and normalized to 2μg of total starting material. Material was then incubated overnight with HDAC3 antibody (CST 85057S) or rabbit IgG

(CST 2729S) and immunoprecipitated with Protein A DynaBeads (Invitrogen 10002D). Assay incubations were performed on-bead with final sample removed from beads for measurement and normalization according to kit instructions.

Chromatin Immunoprecipitation

Chromatin immunoprecipitation (ChIP) was done as previously described with minor modifications (23). Total protein for each sonicated sample was quantified by BCA and normalized to 1.5μg of protein for each ChIP prior to incubation with antibody overnight. 5% input was saved prior to antibody incubation and used as input control. Antibodies used were HDAC3 (Genetex GTX109679) and rabbit IgG (CST 2729S) and immunoprecipitated with BSA blocked Protein A agarose beads (Invitrogen 15918014). ChIP DNA was isolated using phenol/chloroform extraction and treated with RNAse A prior to sequencing library preparation.

ChIP-seq Preparation and Analysis

The NEBNext Ultra II DNA Library Prep Kit for Illumina (NEB #E7645S) with AMPure XP Beads (Beckman Coulter, Inc. #A63881) was used to amplify and size select ChIP DNA. Agilent High Sensitivity DNA Kit (5007-4626) KAPA Library Quantification Kit (KR0405) were used to quantify libraries and fragment sizes prior to sequencing. An n=3 was sequenced for NCoR1/2 Control and NCoR1/2 BAT-dKO groups, n=2 for HDAC3 BAT-KO, and n=1 each for input and IgG. The sequencing was done at the Next-Generation Sequencing Core at the University of Pennsylvania on a NextSeq platform (Illumina) at 100SR for a total of 30 million reads per sample.

FASTQ files were aligned to the GRCm38 (mm10) reference genome using bowtie2 v2.4.2 aligner with the following parameters: -N 1. Duplicate reads were removed

with samtools rmdup. Then tag directories were made with Homer v4.11.1. HDAC3 peaks in Control and NCoR1/2 dKO were called using Homer from pooled replicates, using HDAC3 KO as background. findPeaks was used with default parameters, which sets the cutoff to 4-fold minimum enrichment over the background. Homer's mergePeaks was used to intersect the two peak sets and determine Control-only, NCoR1/2 only, and shared peaks. Motif enrichment analysis in various peak sets was performed with Homer's findMotifsGenome.pl with parameters: -size 200 -S 10 -len 8,10,12,14,16. Enrichment score for a motif was calculated as the fraction of target peaks having the motif divided by the fraction of background regions containing the motif. Genes nearest to the peaks were found with Homer's annotatePeaks.pl.

RNA-seq Preparation and Analysis

We analyzed an n of 4 for each group: NCoR2 Control, NCoR2 BAT-sKO, NCoR1/2 Control, NCoR1/2 BAT-dKO. Isolated RNA from these groups was sequenced at Novogene using an Illumina Platform, PE150, with approximately 30 million reads per sample. For NCoR1 Control (n=4) and NCoR1 BAT-sKO (n=3), libraries were prepared using the TruSeq Stranded Total RNA kit (Illumina) and sequenced at the Next-Generation Sequencing Core at the University of Pennsylvania on the NextSeq 500 platform (Illumina) at 75SR for a total of 20-40 million reads per sample.

RNA-sequencing output, including published HDAC3 BAT-KO data (23), was analyzed in tandem using the DIYTranscriptomics course pipeline (62). Briefly, this pipeline uses Kallisto to align and quantify reads, EnemblDB to annotate data, edgeR to normalize read counts, and Limma to determine DEGs. Cut-offs used for these analyses were a CPM of 1 in a minimum of 4 of 31 total samples to identify a transcript as expressed and a $\log_2$FC>|0.58| and adjusted p-value <0.05 for all DEGs per mouse line. Gene

ontology (GO) analysis for RNA-seq was performed using Enrichr (63) with the top ranked KEGG or GO pathways selected by Enrichr combined score. All heat maps are presented as log_2FC for KO over control per mouse line and were generated in GraphPad PRISM 9.3.1 using output files from the above pipeline.

Western Blot

Whole-tissue BAT lysates were prepared as previously described and quantified by Direct Detect (Millipore) (23). For blotting NCoR1/2, 50μg of protein lysate was loaded per lane, with each lane representing a separate biological replicate. Ladder used was a prestained high range multicolor protein ladder (Thermo Scientific 26625). Wet transfer to PVDF was done overnight, and primary antibodies applied in 5% BSA overnight, all at 4°C. Primary antibodies used were anti-SMRTe (Millipore 06-891, 1:1000), anti-NCoR1 (CST 5948S, 1:1000), and anti-Vinculin (Sigma V9264, 1:5000) with appropriate HRP-linked secondary antibodies (CST, 1:10,000) applied at room temperature for one hour. Blots were revealed using either film or a Bio-Rad ChemiDoc.

Metabolic Phenotyping and Norepinephrine Response

All metabolic phenotyping data were collected using Comprehensive Laboratory Animal Monitoring System (CLAMS, Columbus Instruments) metabolic cages housed within environment-controlled incubators. Norepinephrine response was measured as previously described (23). Briefly, oxygen consumption was measured prior to and for two hours following subcutaneous injection of 1 mg kg^{-1} L-(−)-Norepinephrine (+)-bitartrate salt monohydrate (Sigma A9512) dissolved in sterile 0.9% NaCl above the BAT in anesthetized animals.

Histology

Freshly isolated tissue was fixed overnight in 4% paraformaldehyde at 4°C and dehydrated prior to embedding in paraffin and sectioning at a thickness of 7μm. Slides were prepared with two replicates each for control and KO on a single slide for even processing. Hematoxylin and eosin stain was applied by the IDOM histology core using a standard protocol.

Immunohistochemistry

Immunohistochemistry (IHC) for CD45 (Abcam 208022) and CD68 (Abcam 283654) was performed using a standard IHC protocol. Dilutions used were 1:800 for CD45 and 1:400 for CD68. High pH antigen retrieval solution (Invitrogen 00-4956-58) was applied prior to CD68 staining. Simple Stain Mouse MAX PO (Cosmo Bio NIC-414142F) was used as a secondary stain and revealed with DAB. Slides were then counterstained with Carazzi hematoxylin before mounting in Cytoseal XYL (Thermo Scientific 8312-4). Slides were imaged on a ThermoFisher EVOS FL Auto 2 at 20x magnification, choosing representative areas from 4x imaging.

Immunofluorescence

Immunofluorescence (IF) for Tubb3 (Abcam 52623) and TH (EMD Millipore AB1542) was performed as previously described (17). Dilutions used were 1:200 for TH and 1:800 for Tubb3, with 1:500 used for secondary antibodies. Sections were mounted with DAPI Fluoromount (SouthernBiotech 0100-20) and imaged using a Zeiss Observer 7 at 40x magnification. Fluorescent signal in each image layer was quantified using Fiji automatic signal measurement prior to any adjustment of image brightness or contrast and

normalized to the average of the control signal (64). The final resolution of the 40x images is 1920x1210 with a pixel width of 0.1465 microns.

BAT Fractionation

For stromal vascular fraction isolation, BAT was harvested from adult mice and incubated in a gentleMACS Dissociator (Miltenyi Biotech 130-096-427) with 2.4U/mL Dispase II and 1.5U/mL Type I Collagenase for 40 minutes at 37°C. Lysate was then filtered over a 200uM filter before a gentle spin for 3 minutes at 50g. The adipocyte layer was carefully removed from the top of the lysate before a second spin for 5 minutes at 500g to pellet SVF. Pelleted SVF was then resuspended in Trizol for RNA isolation and quantification.

Primary Brown Adipocyte Culture

Primary brown pre-adipocytes were isolated and differentiated in culture as previously described from BAT of 1-5 day old pups (23). Genotype of pups was either *Rosa26-CreER* positive or negative and all NCoR1/2 floxed. Isolated cells were initially pooled by genotype and tamoxifen applied to all wells from day 0-2 of differentiation. Replicates were differentiated individually in 12-well plates prior to isolation of RNA as described in *Isolation and Quantification of RNA (RT-qPCR)*. Oil Red O staining was done as previously described (65) to confirm differentiation in separate 6-well plates and imaged at 20x on a ThermoFisher EVOS FL Auto 2 microscope.

Statistical Analysis

Statistical analyses were performed using R (version 4.1) for sequencing data (as described in the sequencing analyses sections) and GraphPad Prism (version 9.3) for all other data types. All data with error bars are presented at mean ±SEM with replicates

shown as individual points. Statistical analyses used were unpaired 2-tailed t test for direct comparisons between 2 groups, 2-way analysis of variance (ANOVA) with repeated measures for analysis of 2 groups over time, or a 1-way ANOVA, with Tukey corrected multiple comparisons, for analysis of a single variable between multiple groups. P-values throughout are reported as *p<0.05, **p<0.01, **p<0.001, ***p<0.0001, and ****p<0.00001 with adjusted p-values used where appropriate.

Acknowledgments

We thank C.D. Holman and C.C. Chan for valuable discussions and B.J. Carpenter and B.M. Krusen for assistance with animal husbandry. We are grateful to the L Chang of the Histology Core of the Institute for Diabetes, Obesity, and Metabolism for slide preparation, and to J. Zhao of the Cell and Developmental Biology Microscopy Core for microscopy training and assistance. We also thank the Functional Genomics Core and Rodent Metabolic Phenotyping Core of the and Penn Diabetes Center (DK19525) for next generation sequencing and CLAMS experiments, respectively. This work was supported by NIH R01 DK43806 (M.A.L.), NIH T32 DK007314 and F32 DK122684 (A.K.H), The Uehara Memorial Foundation, Leading Young Researcher Overseas Visit Program and the Osamu Hayaishi Memorial Scholarship for Study Abroad (S-I.I.), the Cox Medical Research Institute, and the JPB Foundation.

References

1. Y. Wang, *et al.*, Has the prevalence of overweight, obesity and central obesity levelled off in the United States? Trends, patterns, disparities, and future projections for the obesity epidemic. *Int. J. Epidemiol.* **49**, 810–823 (2020).

2. A. Ruban, K. Stoenchev, H. Ashrafian, J. Teare, Current treatments for obesity. *Clin. Med.* **19**, 205–212 (2019).

3. L. Cheng, *et al.*, Brown and beige adipose tissue: a novel therapeutic strategy for obesity and type 2 diabetes mellitus. *Adipocyte* **10**, 48–65 (2021).

4. C.-H. Wang, Y.-H. Wei, Therapeutic Perspectives of Thermogenic Adipocytes in Obesity and Related Complications. *Int. J. Mol. Sci.* **22**, 7177 (2021).

5. B. Cannon, J. Nedergaard, Brown Adipose Tissue: Function and Physiological Significance. *Physiol. Rev.* **84**, 277–359 (2004).

6. A. M. Cypess, *et al.*, Activation of Human Brown Adipose Tissue by a β3-Adrenergic Receptor Agonist. *Cell Metab.* **21**, 33–38 (2015).

7. K. L. Townsend, Y.-H. Tseng, Brown Fat Fuel Utilization and Thermogenesis. *Trends Endocrinol. Metab. TEM* **25**, 168–177 (2014).

8. E. T. Chouchani, L. Kazak, B. M. Spiegelman, New Advances in Adaptive Thermogenesis: UCP1 and Beyond. *Cell Metab.* **29**, 27–37 (2019).

9. F. Omran, M. Christian, Inflammatory Signaling and Brown Fat Activity. *Front. Endocrinol.* **11**, 156 (2020).

10. D. A. Hill, *et al.*, Distinct macrophage populations direct inflammatory versus physiological changes in adipose tissue. *Proc. Natl. Acad. Sci. U. S. A.* **115**, E5096–E5105 (2018).

11. H. L. Caslin, M. Bhanot, W. R. Bolus, A. Hasty, Adipose tissue macrophages: unique polarization and bioenergetics in obesity. *Immunol. Rev.* **295**, 101–113 (2020).

12. S. M. Reilly, A. R. Saltiel, Adapting to obesity with adipose tissue inflammation. *Nat. Rev. Endocrinol.* **13**, 633–643 (2017).

13. F. Villarroya, R. Cereijo, A. Gavaldà-Navarro, J. Villarroya, M. Giralt, Inflammation of brown/beige adipose tissues in obesity and metabolic disease. *J. Intern. Med.* **284**, 492–504 (2018).

14. K. Fischer, *et al.*, Alternatively activated macrophages do not synthesize catecholamines or contribute to adipose tissue adaptive thermogenesis. *Nat. Med.* **23**, 623–630 (2017).

15. M.-W. Lee, *et al.*, Activated Type 2 Innate Lymphoid Cells regulate Beige Fat Biogenesis. *Cell* **160**, 74–87 (2015).

16. K. D. Nguyen, *et al.*, Alternatively activated macrophages produce catecholamines to sustain adaptive thermogenesis. *Nature* **480**, 104–108 (2011).

17. B. Hu, *et al.*, γδT cells and adipocyte IL-17RC control fat innervation and thermogenesis. *Nature* **578**, 610–614 (2020).

18. A. C. Kohlgruber, *et al.*, γδ T cells producing interleukin-17A regulate adipose regulatory T cell homeostasis and thermogenesis. *Nat. Immunol.* **19**, 464–474 (2018).

19. C. K. Glass, M. G. Rosenfeld, The coregulator exchange in transcriptional functions of nuclear receptors. *Genes Dev.* **14**, 121–141 (2000).

20. D. M. Lonard, B. W. O'Malley, Nuclear receptor coregulators: modulators of pathology and therapeutic targets. *Nat. Rev. Endocrinol.* **8**, 598–604 (2012).

21. N. Liang, T. Jakobsson, R. Fan, E. Treuter, The Nuclear Receptor—Co-repressor Complex in Control of Liver Metabolism and Disease. *Front. Endocrinol.* **10** (2019).

22. M. G. Guenther, O. Barak, M. A. Lazar, The SMRT and N-CoR Corepressors Are Activating Cofactors for Histone Deacetylase 3. *Mol. Cell. Biol.* **21**, 6091–6101 (2001).

23. M. J. Emmett, *et al.*, Histone Deacetylase 3 Prepares Brown Adipose Tissue For Acute Thermogenic Challenge. *Nature* **546**, 544–548 (2017).

24. H. Yamamoto, *et al.*, NCoR1 is a conserved physiological modulator of muscle mass and oxidative function. *Cell* **147**, 827–839 (2011).

25. J. H. Kahn, *et al.*, SMRT Regulates Metabolic Homeostasis and Adipose Tissue Macrophage Phenotypes in Tandem. *Endocrinology* **161**, bqaa132 (2020).

26. W. Sun, et al., snRNA-seq reveals a subpopulation of adipocytes that regulates thermogenesis. *Nature* **587**, 98–102 (2020).

27. T. Inagaki, J. Sakai, S. Kajimura, Transcriptional and epigenetic control of brown and beige adipose cell fate and function. *Nat. Rev. Mol. Cell Biol.* **17**, 480–495 (2016).

28. A.-S. Laramée, *et al.*, Opposing Roles for the Related ETS-Family Transcription Factors Spi-B and Spi-C in Regulating B Cell Differentiation and Function. *Front. Immunol.* **11** (2020).

29. A. G. Bassuk, J. M. Leiden, “The Role of Ets Transcription Factors in the Development and Function of the Mammalian Immune System” in *Advances in Immunology*, F. J. Dixon, Ed. (Academic Press, 1997), pp. 65–104.

30. H. C. B. Nguyen, M. Adlanmerini, A. K. Hauck, M. A. Lazar, Dichotomous engagement of HDAC3 activity governs inflammatory responses. *Nature* **584**, 286–290 (2020).

31. C. Yu, *et al.*, The Nuclear Receptor Corepressors NCoR and SMRT Decrease Peroxisome Proliferator-activated Receptor γ Transcriptional Activity and Repress 3T3-L1 Adipogenesis*. *J. Biol. Chem.* **280**, 13600–13605 (2005).

32. P. Li, *et al.*, Adipocyte NCoR knockout decreases PPARγ phosphorylation and enhances PPARγ activity and insulin sensitivity. *Cell* **147**, 815–826 (2011).

33. Z. Gerhart-Hines, *et al.*, The nuclear receptor Rev-erbα controls circadian thermogenic plasticity. *Nature* **503**, 410–413 (2013).

34. V. M. Ramakrishnan, N. L. Boyd, The Adipose Stromal Vascular Fraction as a Complex Cellular Source for Tissue Engineering Applications. *Tissue Eng. Part B Rev.* **24**, 289–299 (2018).

35. M. François, *et al.*, Sympathetic innervation of the interscapular brown adipose tissue in mouse. *Ann. N. Y. Acad. Sci.* **1454**, 3–13 (2019).

36. T. J. Bartness, C. H. Vaughan, C. K. Song, Sympathetic and sensory innervation of brown adipose tissue. *Int. J. Obes. 2005* **34 Suppl 1**, S36-42 (2010).

37. R. Watanabe, *et al.*, MMP (Matrix Metalloprotease)-9–Producing Monocytes Enable T Cells to Invade the Vessel Wall and Cause Vasculitis. *Circ. Res.* **123**, 700–715 (2018).

38. Z. Zhang, *et al.*, Non-shivering Thermogenesis Signaling Regulation and Potential Therapeutic Applications of Brown Adipose Tissue. *Int. J. Biol. Sci.* **17**, 2853–2870 (2021).

39. J. Zhang, M. Kalkum, B. T. Chait, R. G. Roeder, The N-CoR-HDAC3 Nuclear Receptor Corepressor Complex Inhibits the JNK Pathway through the Integral Subunit GPS2. *Mol. Cell* **9**, 611–623 (2002).

40. M. J. Emmett, M. A. Lazar, Integrative regulation of physiology by histone deacetylase 3. *Nat. Rev. Mol. Cell Biol.* **20**, 102–115 (2019).

41. Z. Sun, *et al.*, Deacetylase-independent function of HDAC3 in transcription and metabolism requires nuclear receptor corepressor. *Mol. Cell* **52**, 769–782 (2013).

42. S. Ghisletti, *et al.*, Cooperative NCoR/SMRT interactions establish a corepressor-based strategy for integration of inflammatory and anti-inflammatory signaling pathways. *Genes Dev.* **23**, 681–693 (2009).

43. M. G. Guenther, M. A. Lazar, “Biochemical Isolation and Analysis of a Nuclear Receptor Corepressor Complex” in *Methods in Enzymology*, Nuclear Receptors., (Academic Press, 2003), pp. 246–257.

44. Y.-D. Wen, *et al.*, The histone deacetylase-3 complex contains nuclear receptor corepressors. *Proc. Natl. Acad. Sci. U. S. A.* **97**, 7202–7207 (2000).

45. E. Y. Huang, *et al.*, Nuclear receptor corepressors partner with class II histone deacetylases in a Sin3-independent repression pathway. *Genes Dev.* **14**, 45–54 (2000).

46. A. Codina, *et al.*, Structural insights into the interaction and activation of histone deacetylase 3 by nuclear receptor corepressors. *Proc. Natl. Acad. Sci.* **102**, 6009–6014 (2005).

47. P. Kulozik, *et al.*, Hepatic Deficiency in Transcriptional Cofactor TBL1 Promotes Liver Steatosis and Hypertriglyceridemia. *Cell Metab.* **13**, 389–400 (2011).

48. N. Liang, *et al.*, Hepatocyte-specific loss of GPS2 in mice reduces non-alcoholic steatohepatitis via activation of PPARα. *Nat. Commun.* **10**, 1684 (2019).

49. C. T. Cederquist, *et al.*, Systemic insulin sensitivity is regulated by GPS2 inhibition of AKT ubiquitination and activation in adipose tissue. *Mol. Metab.* **6**, 125–137 (2016).

50. Z. Sun, *et al.*, Hepatic Hdac3 promotes gluconeogenesis by repressing lipid synthesis and sequestration. *Nat. Med.* **18**, 934–942 (2012).

51. V. Perissi, *et al.*, TBL1 and TBLR1 phosphorylation on regulated gene promoters overcomes dual CtBP and NCoR/SMRT transcriptional repression checkpoints. *Mol. Cell* **29**, 755–766 (2008).

52. S. Löffek, O. Schilling, C.-W. Franzke, Biological role of matrix metalloproteinases: a critical balance. *Eur. Respir. J.* **38**, 191–208 (2011).

53. K. Kessenbrock, V. Plaks, Z. Werb, Matrix Metalloproteinases: Regulators of the Tumor Microenvironment. *Cell* **141**, 52–67 (2010).

54. F. J. Ruiz-Ojeda, A. Méndez-Gutiérrez, C. M. Aguilera, J. Plaza-Díaz, Extracellular Matrix Remodeling of Adipose Tissue in Obesity and Metabolic Diseases. *Int. J. Mol. Sci.* **20**, 4888 (2019).

55. C. Strieder-Barboza, *et al.*, Depot-specific adipocyte-extracellular matrix metabolic crosstalk in murine obesity. *Adipocyte* **9**, 189–196 (2020).

56. M. A. Gonzalez Porras, *et al.*, Integrins and extracellular matrix proteins modulate adipocyte thermogenic capacity. *Sci. Rep.* **11**, 5442 (2021).

57. G. Berg, M. Barchuk, V. Miksztowicz, Behavior of Metalloproteinases in Adipose Tissue, Liver and Arterial Wall: An Update of Extracellular Matrix Remodeling. *Cells* **8**, 158 (2019).

58. T.-H. Chun, *et al.*, Genetic link between obesity and MMP14-dependent adipogenic collagen turnover. *Diabetes* **59**, 2484–2494 (2010).

59. R. Unal, *et al.*, Matrix Metalloproteinase-9 Is Increased in Obese Subjects and Decreases in Response to Pioglitazone. *J. Clin. Endocrinol. Metab.* **95**, 2993–3001 (2010).

60. H. Shimizu, *et al.*, NCoR1 and SMRT Play Unique Roles in Thyroid Hormone Action In Vivo. *Mol. Cell. Biol.* **35**, 555–565 (2015).

61. S. E. Mullican, *et al.*, Histone deacetylase 3 is an epigenomic brake in macrophage alternative activation. *Genes Dev.* **25**, 2480–2488 (2011).

62. A. S. F. Berry, *et al.*, An Open-Source Toolkit To Expand Bioinformatics Training in Infectious Diseases. *mBio* (2021) https:/doi.org/10.1128/mBio.01214-21 (March 1, 2022).

63. Z. Xie, *et al.*, Gene Set Knowledge Discovery with Enrichr. *Curr. Protoc.* **1**, e90 (2021).

64. J. Schindelin, *et al.*, Fiji: an open-source platform for biological-image analysis. *Nat. Methods* **9**, 676–682 (2012).

65. W. Wang, *et al.*, Ebf2 is a selective marker of brown and beige adipogenic precursor cells. *Proc. Natl. Acad. Sci.* **111**, 14466–14471 (2014).

66. P. J. Watson, L. Fairall, G. M. Santos, J. W. R. Schwabe, Structure of HDAC3 bound to co-repressor and inositol tetraphosphate. *Nature* **481**, 335–340 (2012).

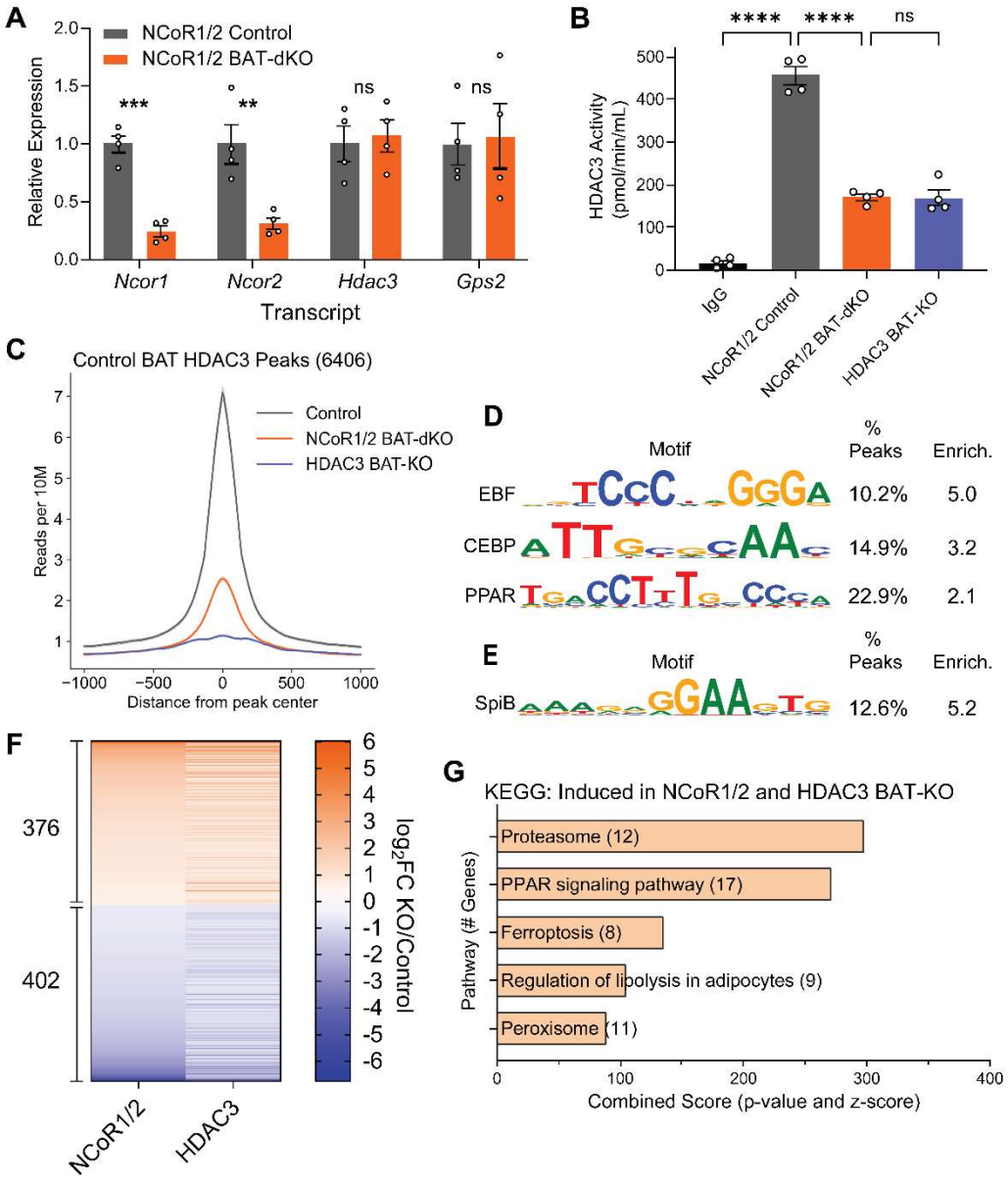

Figure 2.1. HDAC3 canonical function and genomic location requires NCoR1/2. **A**, Gene expression in BAT from NCoR1/2 Control versus NCoR1/2 BAT-dKO littermates housed at thermoneutrality, normalized to housekeeping transcript and control (n=4,4). **B**, HDAC3 activity in BAT lysates, immunoprecipitated with IGG or HDAC3 antibody (n=4 per group). **C**, Average HDAC3 ChIP-seq signal profiles for all HDAC3 peaks (6407) in Control BAT. Shaded area: SEM. **D**, Top enriched known motifs, displaying one example per motif

family, using HOMER in control HDAC3 peak set. **E**, Top enriched known motif using HOMER in HDAC3 peak set from NCoR1/2 BAT-dKO. **F**, Differentially expressed genes (DEGs) shared between NCoR1/2 BAT-dKO and HDAC3 BAT-KO, FC>1.5 up or down, adj.p<0.05 (n=3-4 per group). **G**, KEGG pathways enriched among genes induced in (**F**) highlighting shared regulation of lipid metabolism.

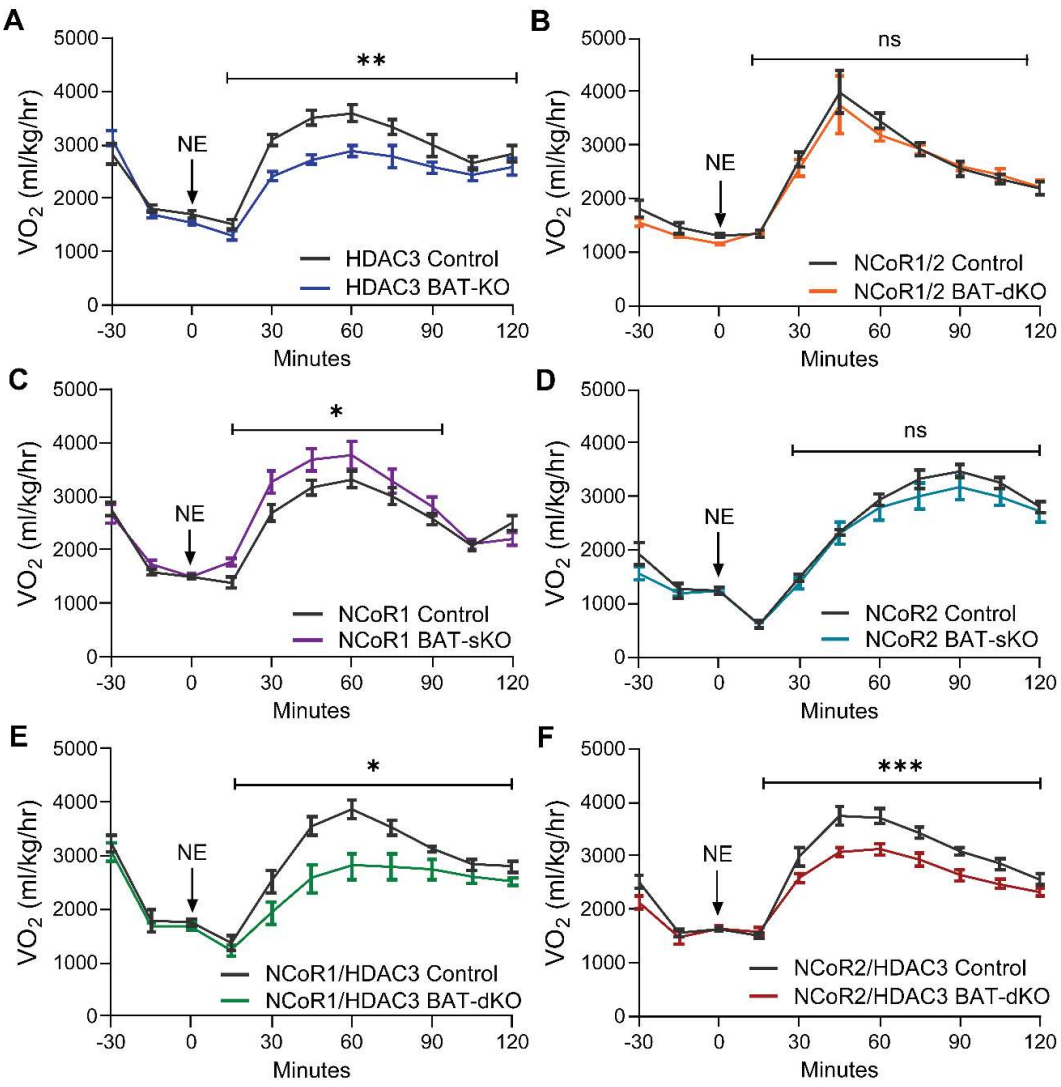

Figure 2.2. NCoR1/2 loss does not phenocopy dominant cold intolerance of HDAC3 loss. **A-F**, Norepinephrine (NE)-induced oxygen consumption following anaesthetization at thermoneutrality, after two weeks of thermoneutral acclimation, for (**A**) NCoR1/2 Control versus BAT-dKO (n=6,6), (**B**) HDAC3 Control versus BAT-sKO (n=5,5), (**C**) NCoR1 Control versus BAT-sKO (n=11,11), (**D**) NCoR1/HDAC3 Control versus BAT-dKO (n=5,5), (**E**) NCoR2 Control versus BAT-sKO (n=5,5), (**F**) NCoR2/HDAC3 Control versus BAT-dKO (n=6,6).

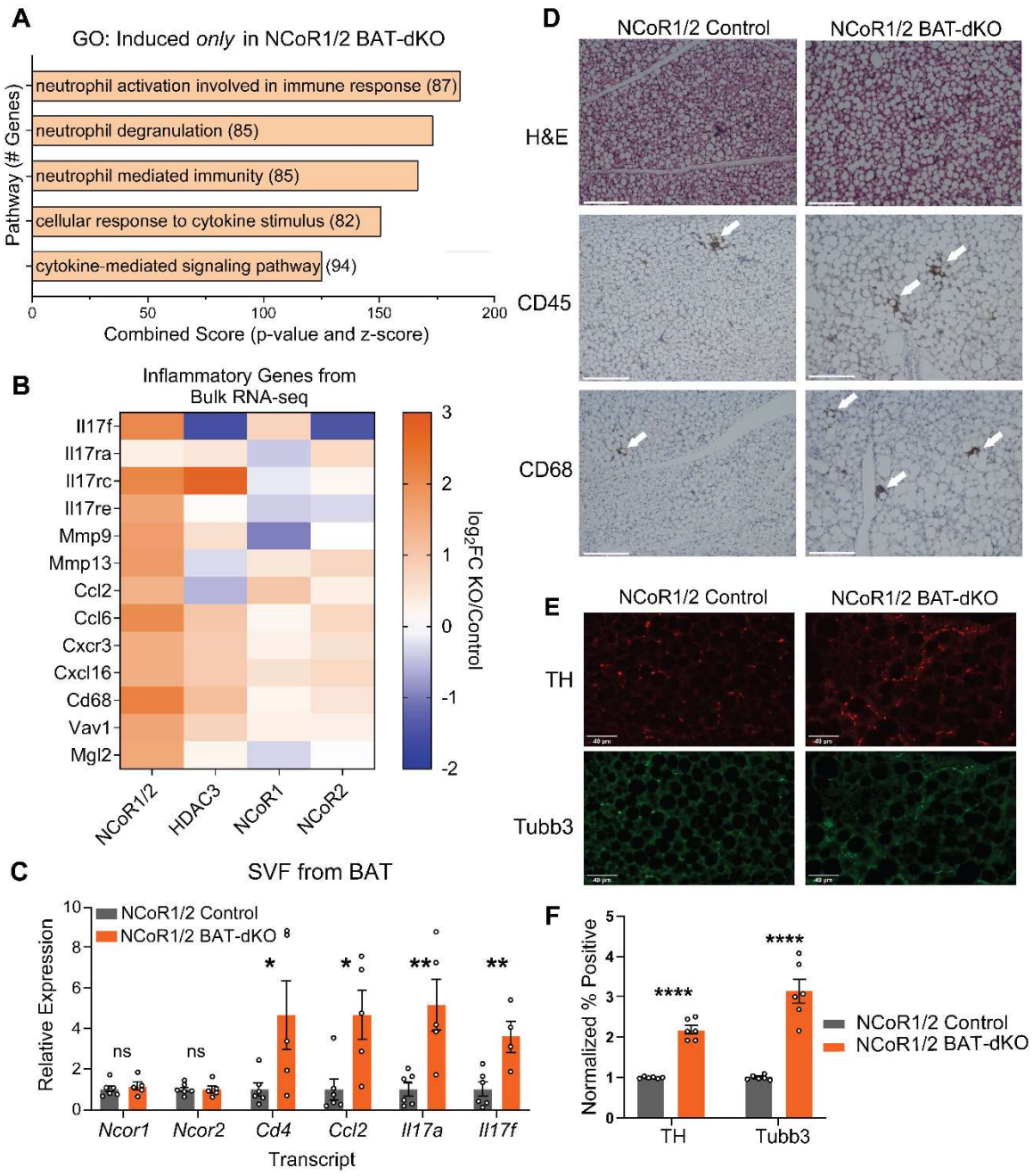

Figure 2.3. IL-17 inflammatory axis mediates NCoR1/2 BAT-dKO phenotype. **A**, Gene ontology terms enriched among DEGs induced only in NCoR1/2 BAT-dKO, highlighting inflammatory regulation. **B**, Heat map of selected inflammatory transcripts related to IL-17 (n=3 per group). **C**, Gene expression in stromal vascular fraction isolated from BAT of NCoR1/2 Control or NCoR1/2 BAT-dKO (n=6,5) **D**, Representative images of H&E, IHC

for CD45, and IHC for CD68 at 20x magnification of BAT from NCoR1/2 Control and NCoR1/2 BAT-dKO, scale bar is 200μM. **E**, Representative images at 40x magnification of IF for TH and Tubb3 in BAT from NCoR1/2 Control and NCoR1/2 BAT-dKO, scale bar is 40μM, **F**, Quantification of fluorescent signal in with six images per group from two biological replicates stained in parallel, normalized to control.

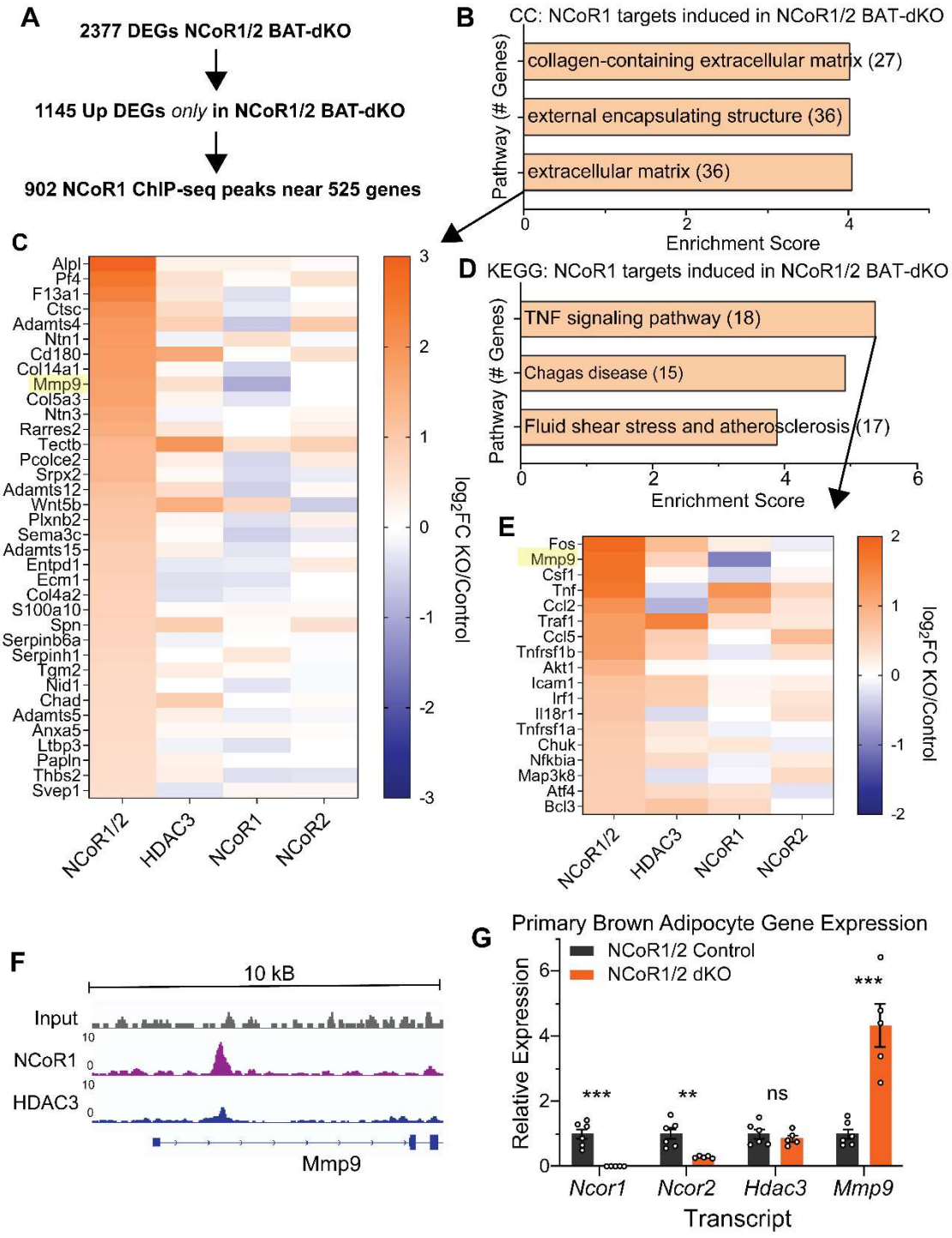

Figure 2.4. Brown adipocyte NCoR1/2 together directly regulate Mmp9. **A**, Schematic of workflow for determining putative direct targets of BAT NCoR1/2. **B**, Cellular component enrichment for 525 NCoR1/2 BAT target genes found in (**A**). **C**, Heat map of extracellular

matrix genes regulated by NCoR1/2 in BAT, Mmp9 highlighted. **D**, KEGG enrichment for 525 NCoR1/2 BAT target genes found in (**A**). **E**, Heat map of TNF signaling pathway genes regulated by NCoR1/2 in BAT, Mmp9 highlighted. **F**, Genome browser tracks for NCoR1 and HDAC3 ChIP-seq in BAT at Mmp9 gene locus, with input control shown. **G**, Gene expression in primary brown adipocytes, either NCoR1/2 Control or NCoR1/2 dKO (n=6,5).

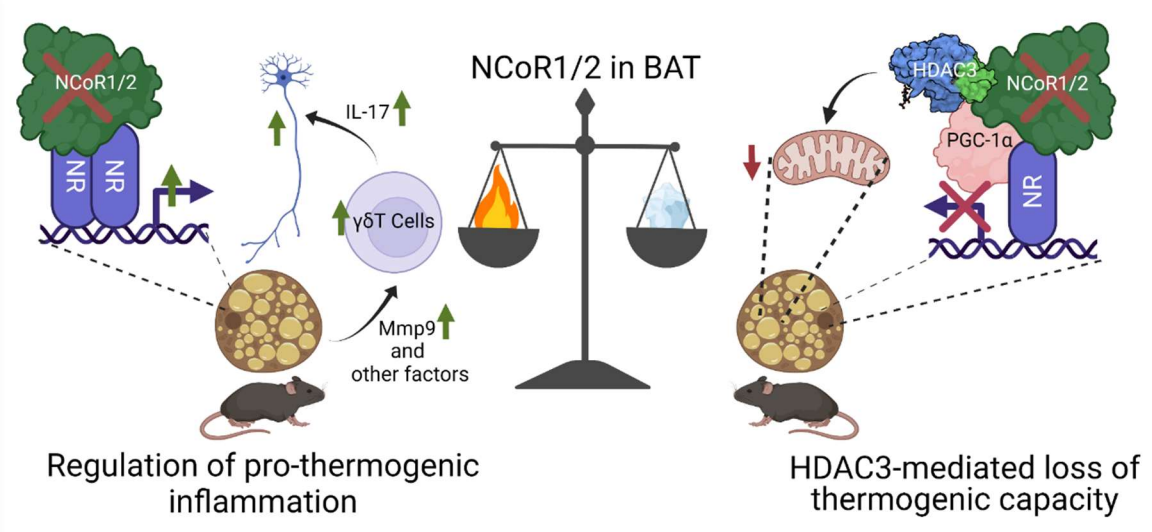

Figure 2.5. Integrated model of NCoR1/2 function in BAT. The functions of NCoR1/2 in BAT balance each other to result in a neutral thermogenic state. On one side is the HDAC3-independent pro-thermogenic inflammatory regulation described in this study with loss of NCoR1/2 in BAT which is offset by the loss of thermogenic capacity via the HDAC3-mediated PGC1-α deacetylation previously described (23). NR: Nuclear Receptor. HDAC3 structure from crystal structure of interaction with NCoR2 (66). Created with BioRender.

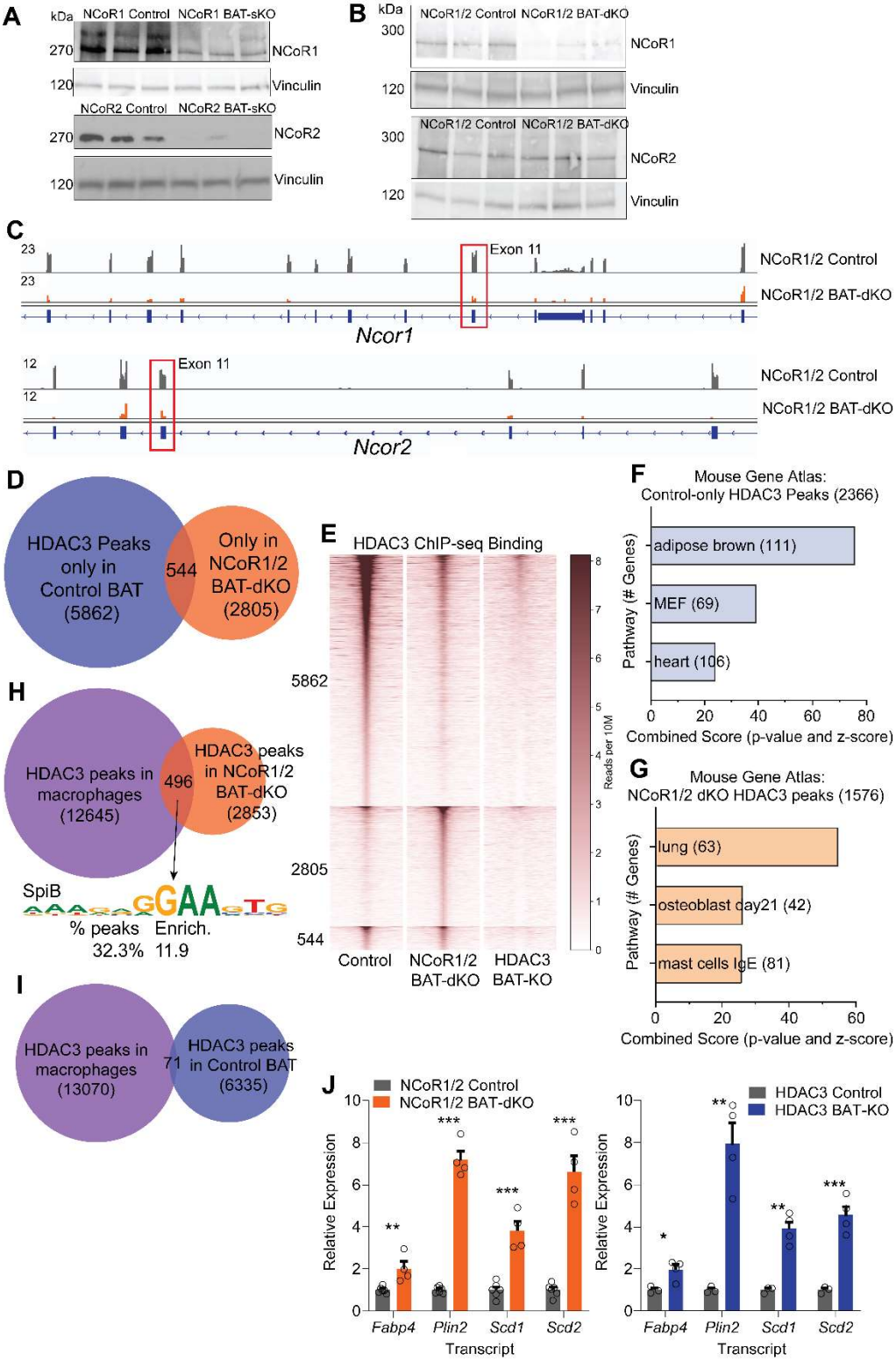
A
kDa
NCoR1 Control
NCoR1 BAT-sKO
270
NCoR1
120
Vinculin
NCoR2 Control
NCoR2 BAT-sKO
270
NCoR2
120
Vinculin
B
kDa
NCoR1/2 Control
NCoR1/2 BAT-dKO
300
NCoR1
120
Vinculin
NCoR1/2 Control
NCoR1/2 BAT-dKO
300
NCoR2
120
Vinculin
C
23
Exon 11
NCoR1/2 Control
23
NCoR1/2 BAT-dKO
Ncor1
12
Exon 11
NCoR1/2 Control
12
NCoR1/2 BAT-dKO
Ncor2
D
HDAC3 Peaks only in Control BAT (5862)
544
Only in NCoR1/2 BAT-dKO (2805)
E
HDAC3 ChIP-seq Binding
5862
2805
544
Control
NCoR1/2 BAT-dKO
HDAC3 BAT-KO
Reads per 10M
F
Mouse Gene Atlas:
Control-only HDAC3 Peaks (2366)
Pathway (# Genes)
adipose brown (111)
MEF (69)
heart (106)
Combined Score (p-value and z-score)
G
Mouse Gene Atlas:
NCoR1/2 dKO HDAC3 peaks (1576)
Pathway (# Genes)
lung (63)
osteoblast day21 (42)
mast cells IgE (81)
Combined Score (p-value and z-score)
H
HDAC3 peaks in macrophages (12645)
496
HDAC3 peaks in NCoR1/2 BAT-dKO (2853)
SpiB
% peaks
32.3%
Enrich.
11.9
I
HDAC3 peaks in macrophages (13070)
71
HDAC3 peaks in Control BAT (6335)
J
NCoR1/2 Control
NCoR1/2 BAT-dKO
Relative Expression
Fabp4
Plin2
Scd1
Scd2
Transcript
HDAC3 Control
HDAC3 BAT-KO
Relative Expression
Fabp4
Plin2
Scd1
Scd2
Transcript

Figure 2.S1. Validation of NCoR1/2 BAT-dKO and HDAC3 binding loss. **A**, Western blots showing loss of either NCoR1 or NCoR2 in brown adipose tissue from the appropriate BAT-sKO model with Vinculin loading control (n=3 per group). **B**, Western blots for NCoR1 and NCoR2 in Control or NCoR1/2 BAT-dKO whole BAT lysate, with Vinculin loading control (n=3,3). **C**, Tracks for RNA quantity from Control and NCoR1/2 BAT-dKO RNA-seq, highlighting floxed exons. **D,** Venn diagram of all HDAC3 peaks called over HDAC3-KO in either Control or NCoR1/2 dKO BAT. **E**, Heat map of peaks from (E), grouped as in (E), and sorted by total signal within groups. **F**, Mouse Gene Atlas enrichment of genes expressed in NCoR1/2 RNA-seq with nearby control BAT HDAC3 peaks. **G**, Mouse Gene Atlas enrichment of genes expressed in NCoR1/2 RNA-seq with nearby HDAC3 peaks in NCoR1/2 BAT-dKO tissue. **H**, Venn diagram of HDAC3 peaks called in macrophages or NCoR1/2 BAT-dKO BAT with top motif identified by HOMER. **I**, Venn diagram of HDAC3 peaks called in macrophages or Control BAT. **J**, Gene expression in BAT for key lipid metabolism transcripts in either Control/NCoR1/2 BAT-dKO (n=6,4) or Control/HDAC3 BAT-KO tissue (n=3,4) housed at thermoneutrality.

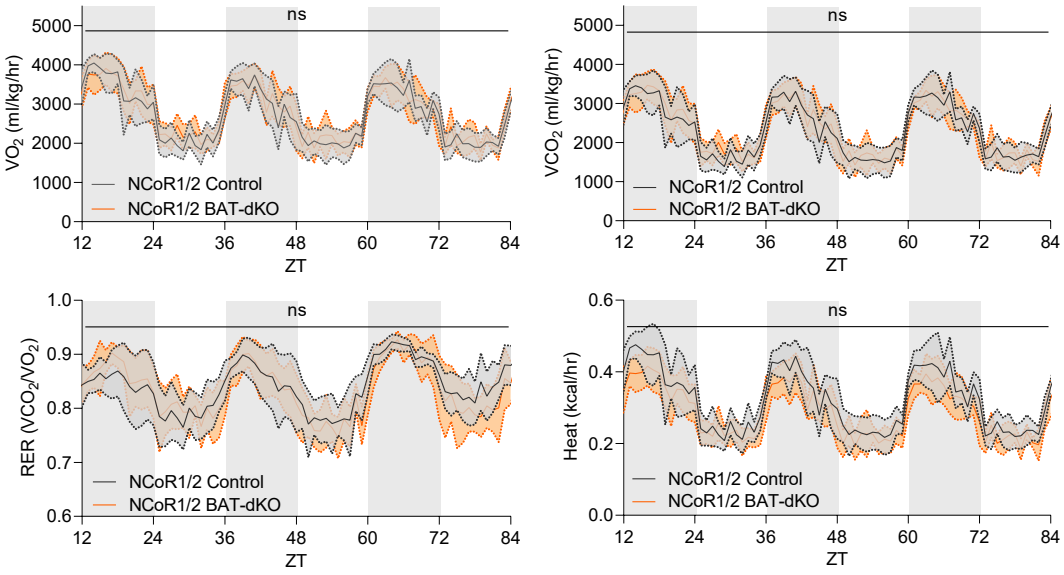

Figure 2.S2. NCoR1/2 in BAT do not regulate basal respiration. VO_2, VCO_2, RER and heat over 72 hours as measured by the CLAMS in Control and NCoR1/2 BAT-dKO animals at thermoneutral conditions (n=6,6). 95% confidence interval is displayed in shaded area between dashed lines and dark periods indicated by grey shaded background. Statistical testing done with 2-way repeated measures ANOVA, ns=no significance between groups. ZT=Zeitgeber time.

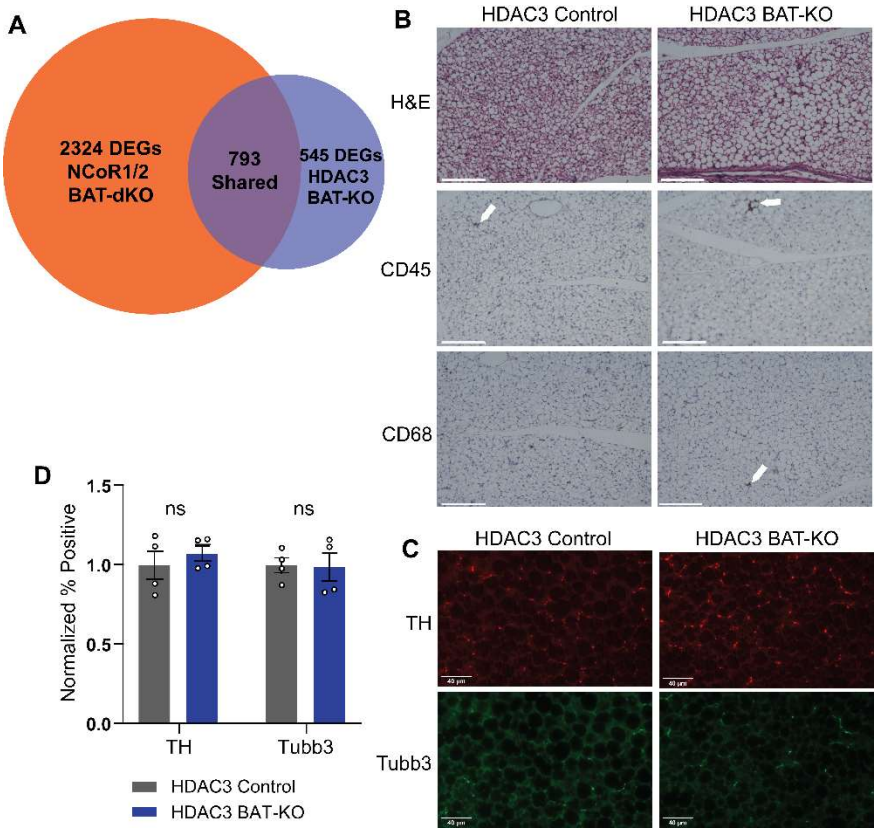

Figure 2.S3. HDAC3 BAT-KO does not show increased inflammation. **A**, Venn diagram of all DEGs from either NCoR1/2 BAT-dKO or HDAC3 BAT-KO. **B**, H&E staining, CD45 and CD68 IHC in HDAC3 Control BAT and HDAC3 BAT-KO, 20x magnification, arrows indicating positive staining, scale bar set to 200μM, **C**, TH and Tubb3 IF staining of HDAC3 Control BAT and HDAC3 BAT-KO, 40x magnification, scale bar set to 40μM, **D**, Quantification of TH and Tubb3 fluorescent signal from four images per group from two biological replicates.

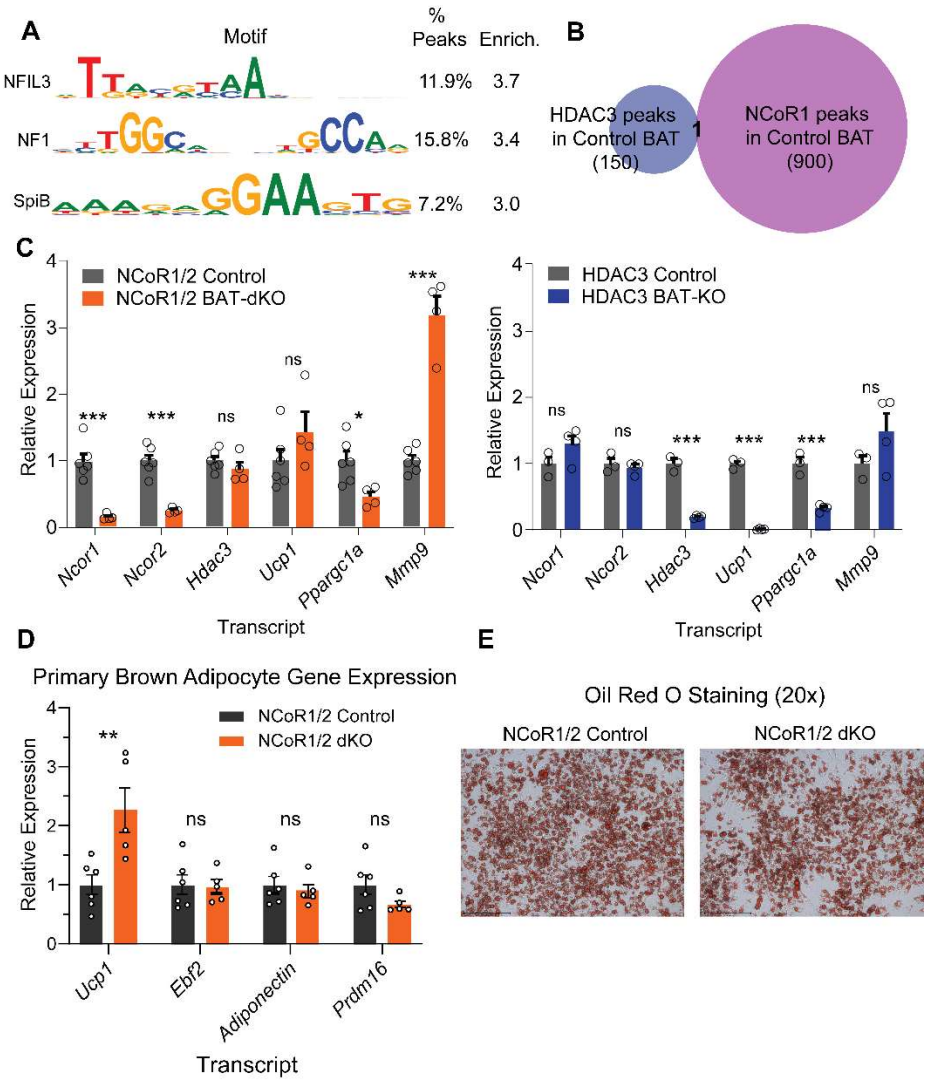

Figure 2.S4. Motif analysis and validation of key transcripts and primary adipocyte system**. A**, Top enriched known motifs, displaying one example per motif family, using HOMER in control NCoR1 peaks near NCoR1/2-regulated genes. **B**, Venn Diagram of all peaks for HDAC3 or NCoR1 in control BAT tissue near NCoR1/2-regulated genes. **C**, Gene expression in BAT from Control/NCoR1/2 BAT-dKO (n=6,4) or Control/HDAC3 BAT-KO tissue (n=3,4) housed at thermoneutrality. **D**, Gene expression in primary brown adipocytes, either NCoR1/2 Control or dKO, of key differentiation markers. **E**, Oil Red O

staining images at 20x magnification of either NCoR1/2 Control or dKO primary brown adipocytes, scale bar is 200μM.

SYBR RT-qPCR		
Gene	**Forward**	**Reverse**
18s	5′-AGTCCCTGCCCTTTGTACACA-3′	5′-CGATCCGAGGGCCTCACTA-3′
Ncor1	5′-TCTGAACAGGAGAATAATGAGAAGCA-3′	5′-GATCCTCCATCAGCCCATTCATAT-3′
Ncor2	5′-TGAGATCATTGATGGCTTGTCTGA-3′	5′-CTTGATCCTCTGCTGGTCCG-3′
Hdac3	5′-CCTGGAACAGGTGACATGTATGA-3′	5′-CGTAAGGGCACATTGAGACAATAG-3′
Gps2	5′-ACCAGCTTCTCGGACTCATCTTCT-3′	5′-GAGGGTGGGCTGGAGCTCTCT-3′
Fabp4	5'-GATGCCTTTGTGGGAACCT-3'	5'-CTGTCGTCTGCGGTGATTT-3'

Plin2	5'-AAGAGGCCAAACAAAAGAGCCAGGAGACCA-3'	5'-ACCCTGAATTTTCTGGTTGGCACTGTGCAT-3'
Scd1	5'-GCTCTACACCTGCCTCTTCG-3'	5'-GCCGTGCCTTGTAAGTTCTG-3'
Scd2	5'-GCATTTGGGAGCCTTGTACG-3'	5'-AGCCGTGCCTTGTATGTTCTG-3'
Cd4	5′-AGTTGTGGGTGTTCAAAGTGACCT-3′	5′-GTGTTTGCACTCTGTCAAGGGG-3′
Ccl2	5′-CTGCCCTAAGGTCTTCAGCAC-3′	5′-AGGCATCACAGTCCGAGTCA-3′
Il17a	5′-CCCTGGACTCTCCACCGCAA-3′	5′-GTGGTCCAGCTTTCCCTCCG-3′
Il17f	5′-CCCGTGAAACAGCCATGGTCA-3′	5′-CCAGGGGAGGACAGTTCCCA-3′
Il17ra	5′-CATCACCACGTGCAGGTCCA-3′	5′-TGCAACTGGCTTGGGAACTGT-3′
Il17rc	5′-TCGAGGCTAGTCTTGGGGCT-3′	5′-AAGACCCCTGCAGTCAGGCA-3′

Mmp9	5′-AGCTCTGCTGCCCCTTACCA-3′	5′-TAGCGGTACAAGTATGCCTCTGC-3′
Ppargc1a	5'-CCCTGCCATTGTTAAGACC-3'	5'-TGCTGCTGTTCCTGTTTTC-3'
Ucp1	5′-ACTGCCACACCTCCAGTCATT-3′	5′-CTTTGCCTCACTCAGGATTGG-3′
Ebf2	5′-GCTGCGGGAACCGGAACGAGA-3′	5′-ACACGACCTGGAACCGCCTCA-3′
Adiponectin	5′-GCACTGGCAAGTTCTACTGCAA-3′	5′-GTAGGTGAAGAGAACGGCCTTGT-3′
Prdm16	5′-CAGCACGGTGAAGCCATTC-3′	5′-GCGTGCATCCGCTTGTG-3′
Genotyping		
Allele	**Forward**	**Reverse**
Ncor1 loxp	5′-TCTGAACAGGAGAATAATGAGAAGCA-3′	5′-GATCCTCCATCAGCCCATTCATAT-3′

Ncor2 loxp	5′-TGAGATCATTGATGGCTTGTCTGA-3′	5′-CTTGATCCTCTGCTGGTCCG-3′
Hdac3 loxp	5′-GCAGTGGTGGTGAATGGCTT-3′	5′-CCTGTGTAACGGGAGCAGAACTC-3′
Ucp1-Cre	5′-GCATTACCGGTCGATGCAACGAGTGATGAG-3′	5′-GAGTGAACGAACCTGGTCGAAATCAGTGCG-3′
Rosa26-CreER	5′-AAAGTCGCTCTGAGTTGTTAT-3′	5′-GGAGCGGGAGAAATGGATATG-3′
Rosa26-CreER, cont.	5′-CCTGATCCTGGCAATTTCG-3′	
Fabp (pos. control)	5′-TGGCATGTGAGGCGGTTAGGTTATCT-3′	5′-GAGCTTTGCCACATCACAGGTCATTC-3′

Table 2.S1. **Primer List.** List of primers used in Chapter 2 for SYBR-based RT-qPCR or genotyping.

CHAPTER 3: Discerning Functions of REV-ERB Nuclear Receptors in BAT

Figure 3.4 and associated text from:

Adlanmerini, Marine, Bryce J. Carpenter, Jarrett R. Remsberg, Yann Aubert, Lindsey C. Peed, **Hannah J. Richter**, and Mitchell A. Lazar. 2019. “Circadian Lipid Synthesis in Brown Fat Maintains Murine Body Temperature during Chronic Cold.” *Proceedings of the National Academy of Sciences* 116 (37): 18691–99. https://doi.org/10.1073/pnas.1909883116.

For Figure 3.4, Hannah J. Richter performed animal husbandry and experiments for REV-ERBα/β DKO mice and helped edit the associated figures and manuscript sections.

Introduction

REV-ERBα, a repressive nuclear receptor of the family NR1D, is required for cell autonomous clock function and was discovered by Dr. Lazar (Lazar et al. 1989). In nearly all cells and tissues, REV-ERBα is expressed with a high amplitude circadian rhythm, such that at ZT22 there is almost no REV-ERBα present (Feng et al. 2011; Balsalobre, Damiola, and Schibler 1998; Gerhart-Hines et al. 2013). Mice lacking REV-ERBα have attenuated troughs in their circadian body temperature rhythms and increased UCP1 expression (Gerhart-Hines et al. 2013), though it is unknown if this effect is due to tissue-autonomous functions of REV-ERBα. REV-ERBα, with its critical role in circadian clocks and high expression in metabolic tissues such as BAT, is a major link between metabolic and

circadian systems (Guan and Lazar 2021), yet its integrative function in energy homeostasis is yet undefined.

REV-ERBβ (NR1D2), also identified as RVR and BD73 (Dumas et al. 1994; Forman et al. 1994; Retnakaran, Flock, and Giguère 1994), has not been studied as well as its close relative REV-ERBα. REV-ERBβ displays a circadian rhythm of expression, though with a lesser amplitude than REV-ERBα (Bugge et al. 2012). Knockout (KO) of REV-ERBβ does not have major effects on the clock or metabolism except when REV-ERBα is also deleted (Bugge et al. 2012; Cho et al. 2012), suggesting that REV-ERBβ primarily functions to back-up REV-ERBα. The function of REV-ERBβ in BAT has not been characterized.

Text below from Adlanmerini et al. 2019:

> "Circadian rhythm of BAT activity regulates circadian body temperature and circadian cold sensitivity (7–11), allowing mammals to live in near-freezing temperature by a profound remodeling of lipid metabolism and an impressive increase in metabolic rate and heat production (12–14). Time-of-day modulation of substrate mobilization and oxidation during acute cold exposure has been reported (8), but the impact of chronic cold exposure on circadian regulation of lipid metabolism in BAT has not been explored to date.
>
> We recently noted that long-term exposure to an obesogenic diet amplified and synchronized circadian rhythms of genes controlling fat synthesis and oxidation in liver, without a similar effect in adipose tissue (15), indicating that chronic noncircadian environmental challenges can alter circadian metabolism in a tissue-specific manner."

Given the unknown nature of REV-ERB function specifically in brown adipose tissue in either thermoneutrality, or chronic cold, we sought to investigate these areas and provide further insight into the coupling of the circadian clock and metabolism. We initially hypothesized that BAT REV-ERBs would have a role in repressing thermogenesis based on the results of the REV-ERBa whole-body KO model (Gerhart-Hines et al. 2013). However, we show here that BAT REV-ERBs do not tissue-autonomously regulate acute

or circadian thermogenesis, though they do regulate the transcription of *Ucp1*. In fact, the core circadian transcriptional output is maintained with loss of REV-ERBs in BAT. Interestingly, REV-ERBs in BAT are rhythmic repressors of *Srebp1* in chronic cold conditions, thereby regulating lipogenesis and fuel availability.

Results

Effective knockout of REV-ERBα/β in BAT leads to derepression of target genes

Nr1d1$^{fl/fl}$/*Nr1d2*$^{fl/fl}$ mice (Dierickx et al. 2019) were bred to either *Ucp1*-Cre or *Adiponectin*-Cre mice and maintained on a C57BL/6J background to generate either REV-ERB BAT-dKO or REV-ERB Adipo-dKO (all adipose) animals with littermate controls. Mice were then housed at thermoneutrality (30°C) for two weeks prior to circadian tissue collection. **Fig. 3.1A** shows RT-qPCR quantification of transcription in BAT over 24 hours, with one time point every 4 hours in either Control or REV-ERB BAT-dKO animals. *Nr1d1* and *Nr1d2*, the transcripts for REV-ERBa/b, show reduction at all time points but especially ZT6-10 where the transcripts peak in control tissue. *Arntl*, the transcript for the primary clock target of REV-ERB, BMAL1, showed 20-fold derepression at ZT10 and overall increase at most time points. *Ucp1* transcription also showed an overall depression at all time points, though only 4-fold even at ZT10. Similar results for BAT from REV-ERB Adipo-dKO animals are shown in **Fig. 3.1B**.

Loss of REV-ERBα/β in BAT does not significantly affect acute or circadian thermogenesis

Given the increase in *Ucp1* expression observed in **Figure 3.1**, we next moved to test if this translated to an increase in thermogenic capacity. A cold-tolerance test is a classic test for acute thermogenesis. In this case we housed animals at thermoneutrality

for 3-4 days to reduce the thermogenic input normally present at room temperature housing, then moved the mice to cold (4°C) at ZT4. **Fig 3.2A** and **B** respectively show hourly core temperature monitoring for control littermates versus REV-ERB BAT-dKO or REV-ERB Adipo-dKO animals. **Fig. 3.2C** and **D** show survival curves for the same experiments as **A-B** where "death" is a drop of 10°C from starting temperature, requiring removal from the experiment. Neither model showed an improvement in thermogenesis, as would be hypothesized based on *Ucp1* expression and prior published data, and mild defect that seems visible is not statistically significant or reproducible.

While **Fig 3.2A-D** test for acute thermogenic capacity, basal circadian thermogenesis is another important function for BAT. To test this, we utilized implantable temperature probes that can then be scanned to check the surrounding temperature, and implanted them directly above the BAT, in control or REV-ERB Adipo-dKO animals housed at room temperature. BAT temperature was then recorded from each individual animal every 15 minutes over 24 hours and is displayed in **Fig 3.2E**. No significant difference was detected in circadian thermogenesis and therefore the experiment was not repeated in the REV-ERB BAT-dKO model.

Major circadian transcription maintained in REV-ERBα/β BAT-dKO

REV-ERBs make up the repressive arm of the molecular clock (**Figure 1.4**), therefore we sought to determine the full transcriptional effect of loss of REV-ERBs in BAT by performing a time-course RNA-sequencing experiment. We therefore sequenced the samples from **Figure 3.1A**, which are BAT tissue from thermoneutrality, collected every 4 hours. We then used JTK_CYCLE to annotate rhythmic transcripts in either control or REV-ERB BAT-dKO samples and found 1262 in Control and 1834 in BAT-dKO with an

overlap of 568 (**Fig. 3.3A**). We checked gene ontology enrichment in the overlapping transcripts, those not affected by loss of REV-ERBs, and saw that circadian terms were highly enriched, indicating that core clock function remained mostly intact (**Fig. 3.3B**). We looked at heat maps for rhythmic transcripts either lost (**Fig 3.4C**) or gained (**Fig. 3.4D**) in this dataset and observed no major difference in rhythm between the sets. Further analysis would be needed to make conclusions about the lost or gained rhythmic transcripts.

Lipogenesis is increased following chronic cold exposure in REV-ERBα/β BAT-dKO mice

Text below from Adlanmerini et al. 2019, with figure numbers adjusted for this chapter.:

"BAT from these REV-ERBα/β BAT double-knockout (DKO) mice was depleted of both REV-ERBα and REV-ERBβ (**Fig. 3.4A and E**), and this had functional consequences including marked de-repression of REV-ERB target genes Ucp1, Bmal1, and Npas2 (**Fig. 3.4B**). Moreover, consistent with the HA-REV-ERBα BAT cistrome and circadian expression, deletion of REV-ERBs increased the expression of Srebp1c and DNL genes expression in BAT of mice exposed to chronic cold temperatures at ZT10 (**Fig. 3.4C**). Together these data suggest that circadian repression by REV-ERBs triggers rhythmicity of Srebp1/DNL gene expression."

"However, opposite to the SCAP-deficient mice, REV-ERBα/β BAT DKO mice maintained their body temperatures longer than control mice during fasting in chronic cold (**Fig. 3.4D**), consistent with the absence of REV-ERBs activating the SREBP/DNL pathway as well as up-regulating uncoupling protein 1 (*Ucp1*)."

Discussion

As neither BAT or adipose tissue-specific REV-ERB dKO models recapitulate the thermogenic increase noted in the REV-ERBα whole-body KO mouse model, other tissues must be contributing to the whole-body results (Gerhart-Hines et al. 2013). One likely candidate is the central nervous system. We know that brown adipose is highly innervated and thermogenesis is under sympathetic nervous system regulation (Yang and

Ruan 2015; Bartness, Vaughan, and Song 2010). This could implicate the hypothalamus, particularly the suprachiasmatic nuclei (SCN) which is known to integrate the clock with many metabolic inputs and outputs (Hastings, Maywood, and Brancaccio 2018). Mice lacking REV-ERBs in the SCN do display a circadian misalignment of heat when placed in dark/dark conditions, however this does not fully explain the light/dark circadian temperature phenotype of the REV-ERBa whole-body mouse (Adlanmerini, Krusen, et al. 2021). Loss of REV-ERBs in the whole hypothalamus does not affect thermogenesis either (Adlanmerini, Nguyen, et al. 2021). Therefore, a tissue beyond the hypothalamus and the BAT is likely contributing to total circadian thermogenesis.

Another organ that is key for integrating circadian rhythms and metabolism is the liver. REV-ERBs in the liver are known to control feeding and the coordination of multiple cell types' circadian alignment (Guan et al. 2020). Additionally, hepatic AKT has been shown to coordinate thermogenesis via FGF21 and WAT lipolysis (Sostre-Colón et al. 2021). While BAT lipolysis is dispensable for classical thermogenesis, lipolysis in both WAT and cardiac tissues is important for full functionality (Shin et al. 2017; Schreiber et al. 2017; Chitraju et al. 2020). Even further, corticosterone levels, as controlled by the adrenal gland are also known to regulate BAT thermogenic capacity (Kroon et al. 2021). Therefore, the liver, the heart, the adrenal gland, and the WAT may all be key contributors to total thermogenic output of the REV-ERBα whole-body KO mouse. Any of these contributions, including those from the CNS, may be small enough to not be noticed in an individual tissue-specific KO, highlighting the importance of considering the entire organism when designing studies to test the regulation of thermogenesis. Potentially, experiments to measure lipolysis, feeding, hormonal levels, and sympathetic innervation could be done in concert with a whole-body KO and multiple tissue-specific KOs to truly

define the integration of thermogenesis and the clock, but this would be a large undertaking.

What these studies also leave open is the role of REV-ERBα/β in BAT at thermoneutral or room temperature conditions. While we have shown that REV-ERBs are not regulating classical thermogenesis in the way hypothesized, that does not mean they do not have another function in the tissue. Further studies of circadian disruption could reveal new avenues to explore. Particularly, the circadian RNA-sequencing data shown in **Fig. 4.3.** could be analyzed by newer methods designed to capture changes in phase angle or phase shifts that are still counted as circadian by JTK_CYCLE analysis (Tackenberg et al. 2018). Additionally, REV-ERB loss in brown adipocytes may be affecting other cell types in the tissue, as with loss of hepatocyte REV-ERBs, which could be investigated using single nuclei sequencing for a transcriptional approach. One other approach, often used in metabolic studies, is to perturb the system by feeding of high fat diet, which has not yet been tried in either adipose REV-ERB dKO system but may yield interesting results, given REV-ERBs' function in lipogenesis in cold conditions.

Together, the results presented in this chapter show that BAT REV-ERBs are not tissue-autonomous regulators of circadian thermogenesis at thermoneutrality. However, BAT REV-ERBs do regulate lipogenesis and fuel availability following chronic cold. These results inform the field about REV-ERB functions in BAT that were previously unknown and open doors to the possible experiments described above. More studies of the integration of the clock and metabolism will continue to be of high interest in a variety of tissues and conditions relevant to human health, be it jetlag or high fat diet.

Materials and methods

Partly adapted from Adlanmerini et al. 2019 and Chapter 2.

Animal husbandry

All animal studies were performed under protocols approved by the University of Pennsylvania Perelman School of Medicine Institutional Animal Care and Use Committee (IACUC). Mice were group-housed in a temperature- and humidity-controlled, specific-pathogen–free animal facility at 22°C under a 12:12-h light–dark cycle with free access to standard chow (LabDiet, 5010 post-weaning; breeding on LabDiet 5021) and water. Mice were moved to an incubator set to 30°C two weeks (14 days) prior to sacrifice or phenotyping unless otherwise noted, with all tissue collection done at the noted ZT or ZT10 if no ZT was given.

Floxed models for *Nr1d1* and *Nr1d2* (Dierickx et al. 2019), were bred to heterozygous *Ucp1*-Cre expressing mice (Jackson Labs, strain:024670) or heterozygous *Adipoq*-Cre expressing mice (Jackson labs, strain: 028020) and maintained on a C57BL/6J background. All experiments were carried out on 11- to 14-wk-old male littermates generated from Cre heterozygous males mated to floxed allele homozygous females, weaned into shared housing.

Isolation and Quantification of RNA (RT-qPCR)

RNA was isolated from snap-frozen BAT as previously described (Emmett et al. 2017) using TRIzol-chloroform extraction followed by RNeasy Mini spin columns (Qiagen) and on-column DNase-digestion

(Qiagen). RNA from cell culture was isolated using the RNeasy Mini kit protocol (Qiagen). Between 1-2mg of total RNA was reverse transcribed to cDNA using a HighCapacity cDNA Reverse Transcription kit (Applied Biosystems). RT-qPCR was performed using

standard curve-based normalization and Power SYBR Green PCR Master mix on the Quant Studio 6 Flex Real-Time PCR system (Applied Biosystems), with all transcripts further normalized to *18s* quantity (**Figure 3.1**) or *36B4* quantity (**Figure 3.4**) and average expression in the control group at ZT10. Biological replicates shown in bar graphs. See primer table (**Table 3.1**) for specific primer sequences.

Cold Tolerance Testing

Testing of cold tolerance was done as previously described (Emmett et al. 2017; Gerhart-Hines et al. 2013). Briefly, animals were acclimated to thermoneutrality (30°C) for 3-4 days prior to movement to cold (4°C) at ZT4 and temperature was monitored by rectal probe every hour for 6 hours or until a drop of 10°C body temperature from start. Mice in the cold were single housed with free access to food and water, but no nestlet available.

Circadian Measurement of BAT Temperature

Experiments were performed with assistance from the University of Pennsylvania Mouse Phenotyping, Physiology and Metabolism Core. Briefly, pill-sized temperature probes were implanted surgically subcutaneously above the BAT. Mice were given a full week to recover from surgery prior to housing in CLAMS and scanning of the probes every 15 minutes for 24 hours to generate a circadian time course of BAT temperature.

Cold Exposure and Core Body Temperature Measurements.

Applies to **Figure 3**: Mice acclimated at 22°C were placed in single-housed cages at 4 to 5 °C or 29 °C for 1 wk. After 5 to 6 d in cold, rectal temperatures were recorded as previously described (53). For the fasting experiments in the cold, mice were housed for 6 d at 4 °C, and the food was removed for 5 to 6 h at ZT1 (8 AM) on day 7.

Western Blot.

BAT samples were homogenized as previously described (Emmett et al. 2017). Western blot images were images using Bio-Rad ChemiDoc Imaging Systems and analyzed by Image Lab software (v5.2). Antibodies used: REV-ERBa (Cell signaling, 2124, 1:1000), REV-ERBb (SantaCruz, sc-398252, 1:1000), and Vinculin (Sigma, V9131, 1:1000).

Circadian RNA-sequencing

Circadian RNA-sequencing was performed by MedGenome at PE150 and a depth of 40M in Total Reads (20M F/20M R) per sample, using samples from the data presented in **Figure 3.1**. An n=3 per timepoint and group was sequenced though one ZT02 Control sample did not cluster and was removed from further analyses. Analyses were performed using standard RNA-seq alignment and processing followed by JTK_CYCLE as previously described (Guan et al. 2020).

Acknowledgements

This work was supported by NIH R01DK45586, the JPB Foundation, and the Cox Institute for Medical Research (to M.A.L.). Bioinformatics for this chapter were performed by Nagaswaroop Nagaraj and chronic cold experiments were conceptualized, executed, and analyzed by Marine Adlanmerini.

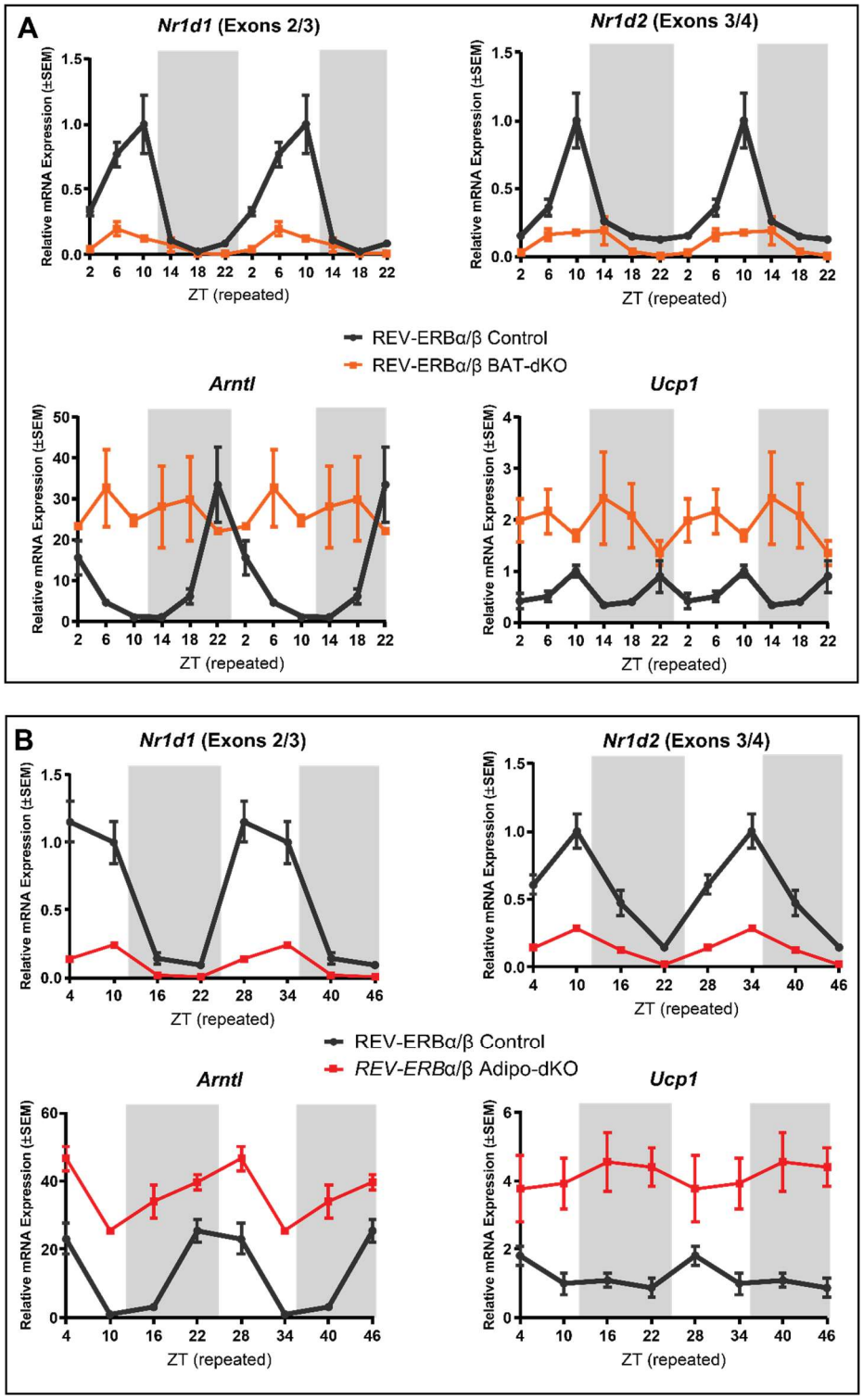

Figure 3.1. Effective knockout of REV-ERBα/β in BAT leads to derepression of target genes. **A**. BAT gene expression over 24 hours (duplicated for visibility) for *Nr1d1,*

Nr1d2, Arntl, and *Ucp1* in control and BAT-dKO, n=3-5 per time point per group. **B**. BAT gene expression over 24 hours (duplicated for visibility) for *Nr1d1, Nr1d2, Arntl,* and *Ucp1* in control and Adipo-dKO, n=4 per time point per group. All samples collected at given ZT following 14 days of thermoneutral (30°C) housing. All samples normalized to *18s* and then control result at ZT10.

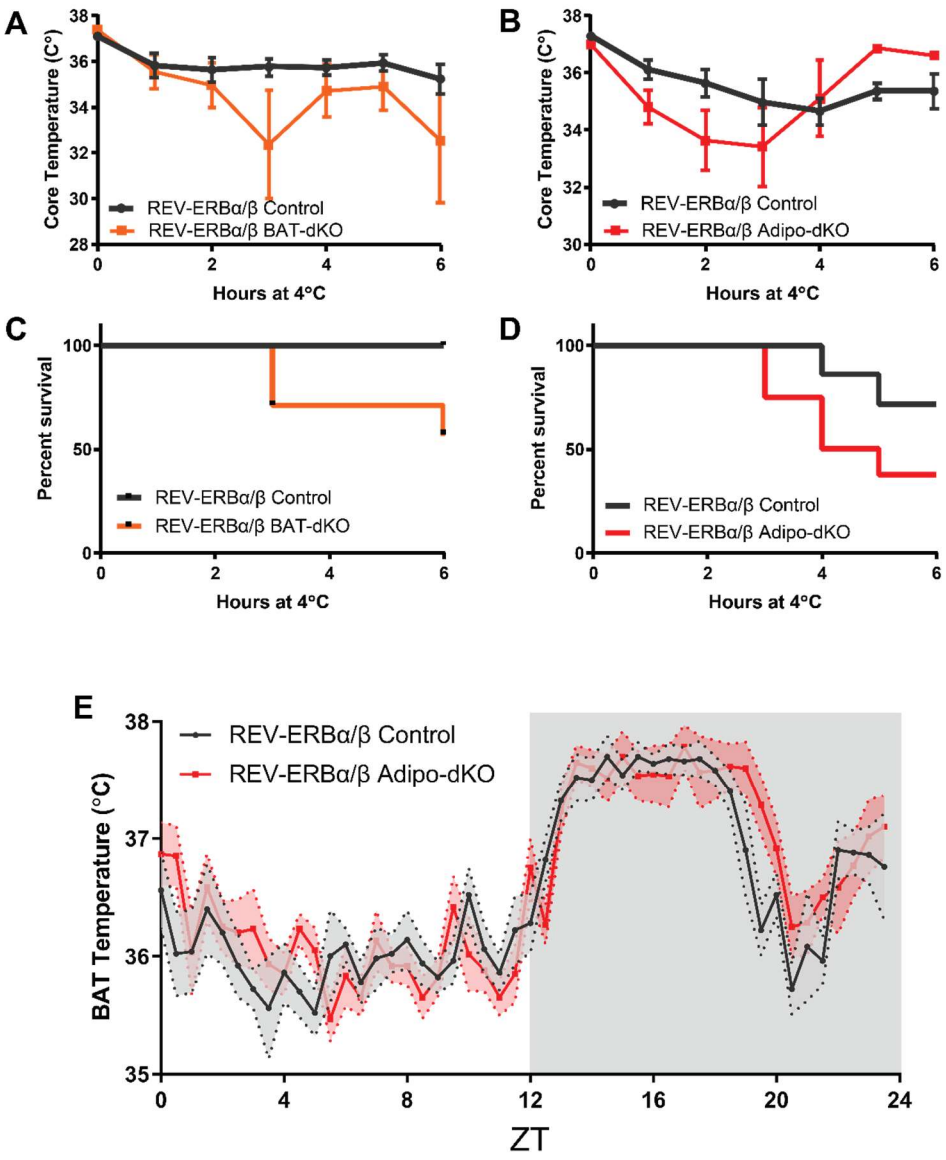

Figure 3.2. Loss of REV-ERBα/β in BAT does not significantly affect acute or circadian thermogenesis. **A**. Core temperature measurement during cold exposure (4°C) following 4 days housed at thermoneutrality (30°C), n=6,7. **B**. Core temperature measurement during cold exposure (4°C) following 3 days housed at thermoneutrality (30°C), n=7,8. **C.** Percent survival for (**A**). **D.** Percent survival for (**B**). **E**. BAT temperature over the course of 24 hours measured using an implantable probe, showing SEM in shaded area, n=5,5.

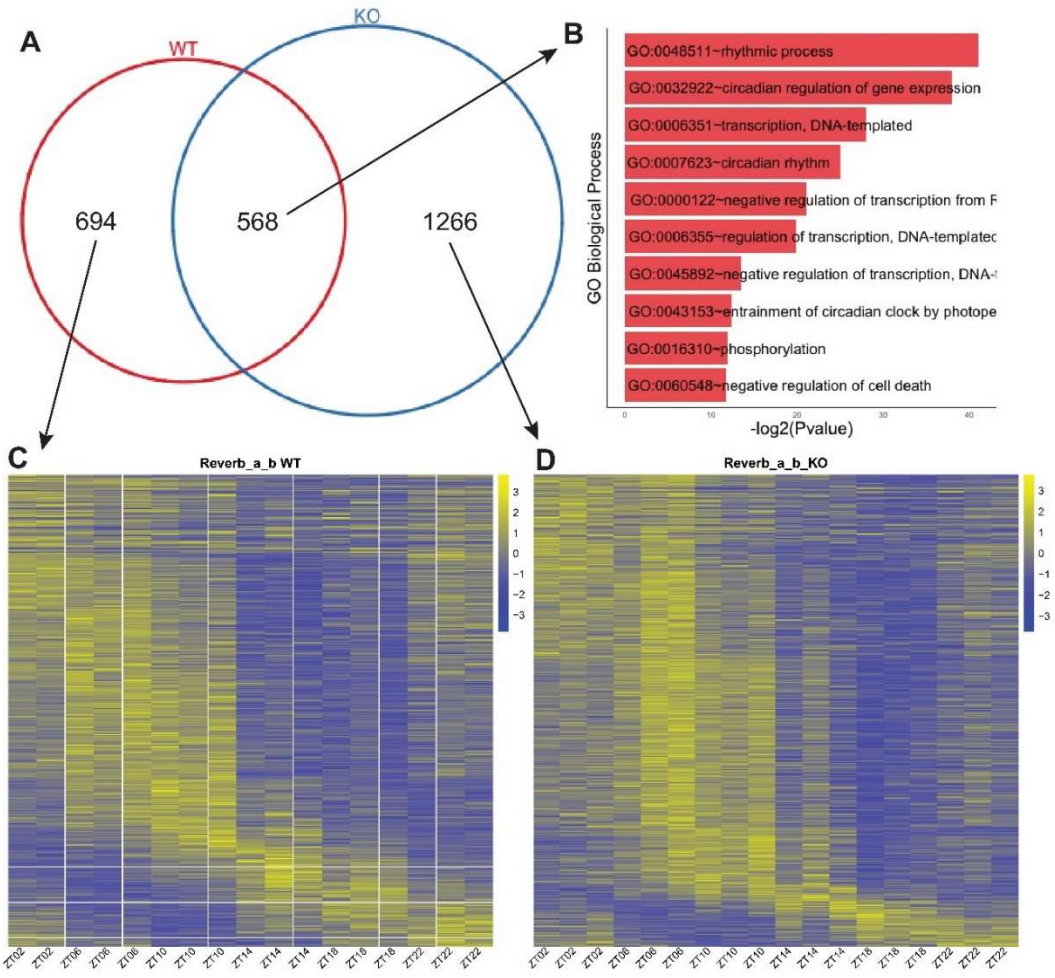

Figure 3.3. Major circadian transcription maintained in REV-ERBα/β BAT-dKO. A. Venn diagram of oscillating transcripts identified using JTK_CYCLE in Control (WT) or REV-ERBa/b BAT-dKO (KO) samples, **B**. Gene ontology showing top enriched pathways in transcripts that are oscillating in both Control and dKO conditions. **C**. Heat map of transcripts oscillating only in Control samples. **D**. Heat map of transcripts oscillating only in REV-ERBa/b BAT-dKO samples. Scale is relative expression for **C** and **D**.

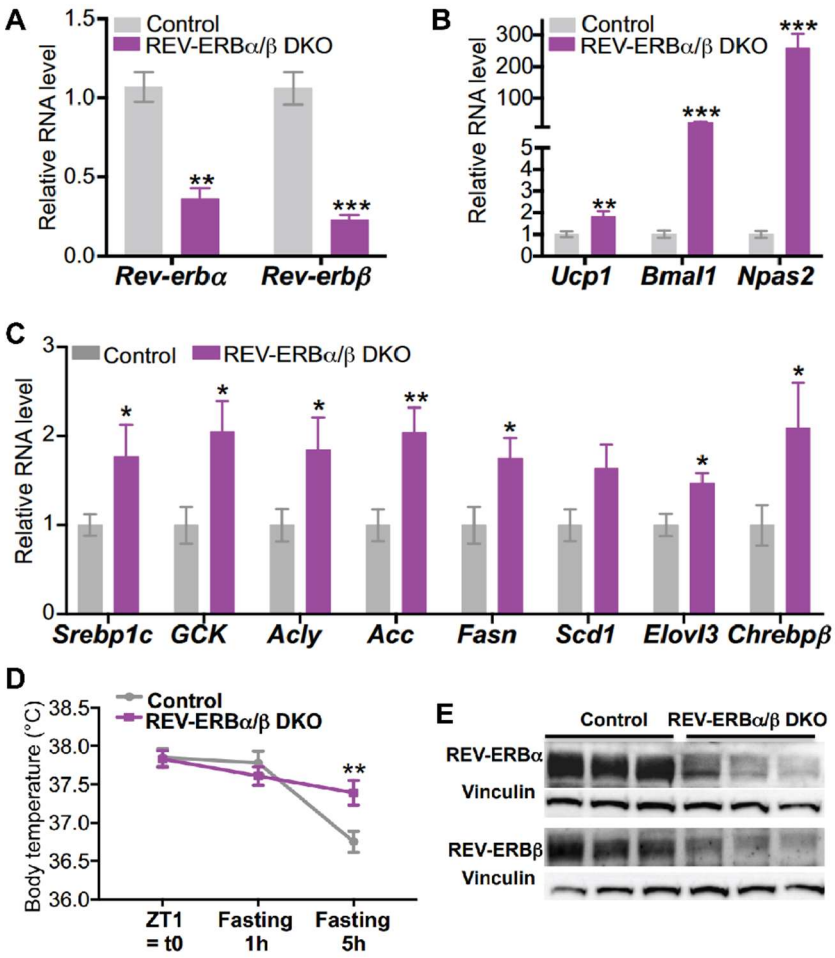

Figure 3.4. Lipogenesis is increased following chronic cold exposure in REV-ERBα/β BAT-dKO mice. A-C. Gene expression in BAT from 1 week at 4°C from either Control or REV-ERBa/b BAT-dKO mice (n=3,3) for either (**A**) knockout confirmation, (**B**) known target genes, or (**C**) lipogenesis genes. **D.** Core temperature of Control or REV-ERBa/b BAT-dKO mice after removal of food availability following housing for 1 week at 4°C (n=10,10). **E**. Western blots showing loss of REV-ERBa and REV-ERBb protein in BAT from mice housed 1 week at 4°C with Vinculin loading control (n=3,3). From Figures 3, 6, and S4 in "Circadian lipid synthesis in brown fat maintains body temperature during chronic cold in mice" (Adlanmerini et al. 2019).

Gene	Forward	Reverse
18s	5′-AGTCCCTGCCCTTTGTACACA-3′	5′-CGATCCGAGGGCCTCACTA-3′
36B4	5′-TCATCCAGCAGGTGTTTGACA-3′	5′-GGCACCGAGGCAACAGTT-3′
Nr1d1	5′-GTCTCTCCGTTGGCATGTCT-3′	5′-CCAAGTTCATGGCGCTCT-3′
Nr1d2	5′-TCATGAGGATGAACAGGAACC-3′	5′-GAATTCGGCCAAATCGAAC-3′
Acc	5′-AAGGCTATGTGAAGGATGTGG-3′	5′-CTGTCTGAAGAGGTTAGGGAAG-3′
Acly	5′-AAGAAGGAGGGGAAGCTGAT-3′	5′-TCGCATGTCTGGGTTGTTTA-3′
Arntl	5′-TAGGATGTGACCGAGGGAAG-3′	5′-TCAAACAAGCTCTGGCCAAT-3′
Chrebpb	5′-TCTGCAGATCGCGTGGAG-3′	5′-CTTGTCCCGGCATAGCAAC-3′
Elovl3	5′-ATGCAACCCTATGACTTCGAG-3′	5′-ACGATGAGCAACAGATAGACG-3′

Fasn	5′-AAGTTCGACGCCTCCTTTTT-3′	5′-TCTCGGGATCTCTGCTAAGG-3′
GCK	5′-TGATGCTGGTGAAAGTGGG-3′	5′-CCAGGAAGTCAGAGATGCAC-3′
Npas2	5′-ATGTTCGAGTGGAAAGGAGAC-3′	5′-CAAGTGCATTAAAGGGCTGTG-3′
Scd1	5′-GCCCCTACGACAAGAACATT-3′	5′-CATGCAGTCGATGAAGAACG-3′
Srebp1c	5′-GGAGCCATGGATTGCACATT-3′	5′-GGCCCGGGAAGTCACTGT-3′
Ucp1	5′-ACTGCCACACCTCCAGTCATT-3′	5′-CTTTGCCTCACTCAGGATTGG-3′

Table 3.1. Primer List. List of primers used in Chapter 3 for SYBR-based RT-qPCR.

CHAPTER 4: Summary

Discussion

One major concern for the field of brown adipose physiology, and specifically for my work, is new knowledge regarding the specificity of *Ucp1*-Cre. While it may have been the best Cre line available to study BAT when this work began, a recent publication has shown that *Ucp1*-Cre is expressed in the brain, kidney, and adrenal glands in development and in the CNS in adult mice (Claflin et al. 2022). This calls into question any results utilizing this Cre line as having possible side effects that were not checked for, since the research community was unaware of these additional expression sites. In the future, other methods of genetically affecting BAT will likely be necessary to at least confirm any major findings originating from *Ucp1*-Cre lines.

Additional options exist, though none as simple as breeding or as (thought to be) specific as *Ucp1*-Cre. One classical option is to also use *Adiponectin*-Cre, which is expressed in all adipose tissues. While this clearly introduces new potential side effects originating in WAT, if the BAT effect is similar to it is with *Ucp1*-Cre it strengthens the likelihood that such effects originate in the BAT rather than in the CNS or elsewhere. If only studying interscapular BAT in adult mice and not whole-body metabolism, other BAT depots, or development, a new method called BAd-CRISPR would be an excellent option for specific depletion of the target of interest (Romanelli et al. 2021). *Ucp1*-CreER mice are also available, allowing bypass of the developmental expression elsewhere with *Ucp1*-Cre by administering tamoxifen to adult mice and using a short timepoint to mitigate CNS effects as tamoxifen does readily cross the blood-brain barrier. No option is perfect, but each could be used to check specific hypotheses arising from *Ucp1*-Cre based data.

Another aspect of this dissertation is the direct connection between the content of Chapters 2 and 3. REV-ERBα is known to recruit the HDAC3-containing corepressor complex, with an *in vitro* preference for NCoR1 over NCoR2 (X. Hu, Li, and Lazar 2001; Yin and Lazar 2005). This allows REV-ERBs to directly repress target gene expression at its binding sites and by mediating looping (Kim et al. 2018). REV-ERBs also mediate gene expression by competing for binding sites with Retinoic Acid-Related Orphan Receptors (RORs) (Solt, Kojetin, and Burris 2011). The circadian distribution of REV-ERBs, RORs, and corepressors at ROR response elements (ROREs) is summarized in **Figure 4.1**. One area of interest for future work may be the functions of the corepressor complex members both in general circadian rhythm regulation and specifically their functions at ZT22 when REV-ERB is absent, and the corepressors are therefore free to redistribute to other sites either together or separately.

While we know from Chapter 3 that REV-ERB targets include both clock genes and metabolic genes, two key clock targets of REV-ERB with validated RORE sites are brain and muscle ARNT-Like 1 (BMAL1, *Arntl*) and Neuronal PAS domain protein 2 (NPAS2, *Npas2*) (Solt, Kojetin, and Burris 2011). Based on the varied levels of induction of these direct targets, and REV-ERBα itself (*Nr1d1*), in the corepressor BAT-KO models presented here, I posit that REV-ERBs are NRs that can bind either NCoR1 or NCoR2 when necessary. *Arntl* is induced strongly with loss of NCoR1, however it is also induced with loss of NCoR2 and most strongly induced with loss of both or HDAC3 (**Figure 4.2**). Additionally, *Npas2* is by far most strongly induced with loss of NCoR1/2, indicating both are responsible for its regulation by REV-ERBs. Therefore, circadian regulation may be most interesting to study in the NCoR1/2 BAT-dKO, rather than either sKO model. Though this hypothesis that either NCoR1/2 can bind REV-ERB *in vivo* would need to be

confirmed by further protein purification techniques such as Co-IPs and the NCoR1/2 ChIP-seq experiments described below.

Future Directions

As with all projects, there are many experiments that I would have loved to accomplish, given more time and better reagents. Hopefully my colleagues will continue to work to better understand the contributions of corepressors and REV-ERBs to brown adipose tissue physiology. Here I discuss just a few next steps that would start to answer those questions left open by my dissertation work.

First and foremost, a high-quality ChIP-seq data set for NCoR2 in BAT would solidify many of the claims made in Chapter 2, particularly those centered around Figure 2.4. For the analyses in that section, I was only able to integrate ChIP data for NCoR1 to determine potential direct targets of NCoR1/2 distinct from those of HDAC3. The current commercial antibodies for NCoR2 are not good enough for quality ChIP-sequencing, even with a NCoR2 KO background control; I did attempt this during my dissertation work, but the results were poor. The Lazar lab has recently utilized CRISPR-Cas9 to generate epitope tagged proteins *in vivo* (Adlanmerini et al. 2019; Shabtai et al. 2021). An endogenous epitope tag is an excellent tool for any protein-based experimental work, especially ChIP followed by either sequencing or mass spectrometry. Dr. Amy Hauck is currently pursuing this approach for NCoR2.

Once the NCoR2 ChIP is possible, there are several questions that would be of interest to the field. First, one could examine overlap between NCoR1/NCoR2/HDAC3 peaks at various gene sets and follow this with motif analysis to find novel candidates that recruit these corepressors individually or as sub-complexes. Second, to test the hypothesis is that NCoR1/2 can compensate for each other at some sites but not others,

one could perform NCoR1/2 ChIPs in the opposite KO background to see how binding changes compared to control at relevant sites.

Other ChIP-sequencing related experiments could also be useful in better understanding exactly how the corepressors are regulating gene expression. Histone marks can be used to understand where active enhancers or promoters lie in the genome and can be modified by active HDAC3. Therefore, ChIP-seq for H3K27ac and H3K9ac would be of interest to perform in the various corepressor BAT-KO models to narrow down peaks and understand if loss of various corepressor subunits is affecting local acetylation states. Of course, acetylation can also be added by histone acetyltransferases (HATs). Therefore, ChIP-seq for key HATs, such as CBP and p300, again in the various corepressor BAT-KO models, would help understand if redistribution of HATs is occurring with loss of the corepressors. For example, it is possible that some of the genes increased in the NCoR1/2 BAT-dKO are regulated by an increase in HAT recruitment given that any nuclear receptors present at regulatory sites cannot recruit the HDAC3 corepressor complex, as related to a coregulator exchange or shift model (Glass and Rosenfeld 2000; Shabtai et al. 2021).

Another area left open by the data presented in Chapter 2 is the exact immune cell (or other cell type) composition of the BAT in response to loss of NCoR1/2. While we propose there that an IL-17 inflammatory axis is induced, including the cytokines and various immune cell markers, this is not a precise way of determining immune cell infiltration. The simpler of two approaches to this problem, and the more targeted approach, is to do flow cytometry on the isolated SVF fraction, using antibodies for $\gamma\delta$T cell surface markers or any other immune cell types. This must be done on just the SVF as adipocytes are generally too large to be sorted in a standard flow cytometry set-up.

An option that may be more appealing, given it is untargeted and may provide other data of interest, is to do single nuclei RNA-sequencing on control and NCoR1/2 dKO-BAT. Again, because adipocytes are large, traditional single cell methods with flow cells do not accommodate them. Therefore, newer methods use nuclei extraction followed by a modified single cell barcoding approach to get a true profile of transcription in adipose tissue cell types (Van Hauwaert et al. 2021). This has been very successful, even in human samples (Sun et al. 2020). This would not only show the presence or absence of specific immune populations in the NCoR1/2 BAT-dKO but allow analysis of cell-cell communication through methods such as a ligand-receptor map potentially shedding light on the question of how a KO in adipocytes leads to immune infiltration (Armingol et al. 2021).

Also in Chapter 2, we did not ourselves prove that the IL-17 axis and γδT cells were responsible for any improvement in thermogenesis that equalized the phenotype of the NCoR1/2 BAT-dKO mice. We instead cited two papers showing a function for γδT cells and IL-17A/F in thermogenic functions (Kohlgruber et al. 2018; B. Hu et al. 2020); both studies relied on loss-of-function models showing a reduction in thermogenic capacity while we posit a positive relationship with increased IL-17A/F. Note that while these studies distinguish between IL-17A and IL-17F, both cytokines are induced in the NCoR1/2 BAT-dKO. To truly test this in our system would not be simple. A long-term option would be to breed our NCoR1/2 dKO-BAT mice with, as one example, the whole-body Tcrδ$^{-/-}$ mice used in Hu et al. that lack γδT cells. If our hypothesis is the entire positive arm of thermogenesis in the NCoR1/2 dKO-BAT mice, these new mice would closely phenocopy the HDAC3 KO mice. However, the Tcrδ$^{-/-}$ mice already have a thermogenic defect, as do the other KO models used in the studies cited, so it would be imperative to

fully check the phenotype and transcriptional effects to make a conclusion.

Given the unexpected nature of the NCoR1/2 BAT-dKO phenotype, one may wonder what the total functions of the core corepressor complex are. To that end, I began breeding triple floxed mice for NCoR1/NCoR2/HDAC3 with either *Ucp1*-Cre, for BAT, or *Rosa26*-CreER, for tamoxifen-induced KO *in vivo* or *ex vivo*. While unable to complete this breeding during my dissertation, I look forward to this reagent being used in the future in comparison with the single and double KOs to uncover the full effects of the HDAC3 corepressor complex on physiology and transcription.

Overall, there is still much to be learned about the relative contributions of NCoR1, NCoR2, and HDAC3 to many aspects of physiology in many organs. Because these corepressors can interact with many nuclear receptors (including REV-ERBs) and the epigenetic landscape, both of which vary by tissue and development stage and circadian time point, there are many niches where these corepressors may be performing important functions. This work only presents a small portion of what new functions we can uncover with careful work using functional *in vivo* approaches.

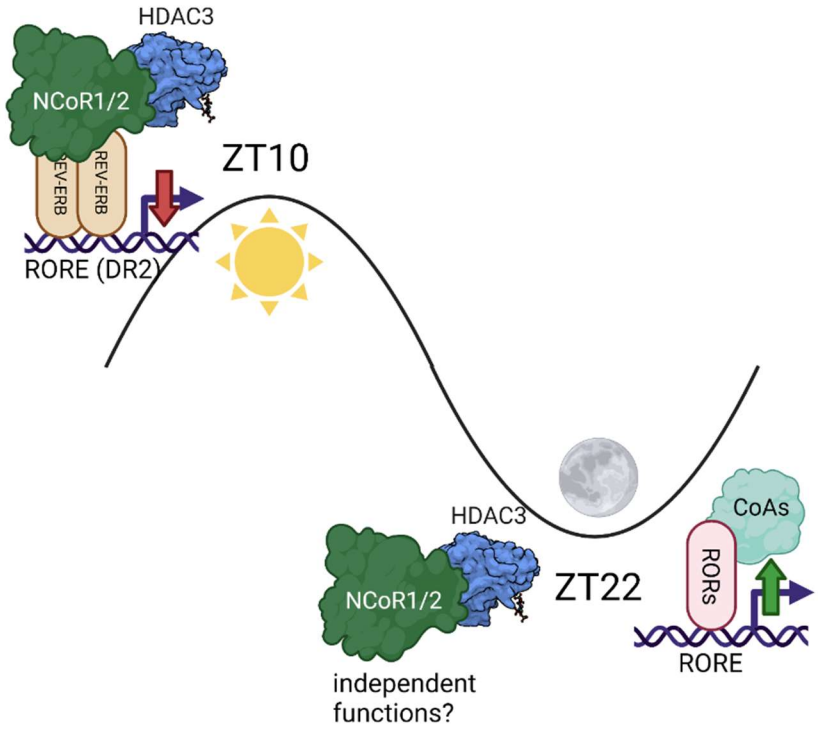

Figure 4.1. Circadian distribution of corepressors at ROR response elements (ROREs). Zeitgeber time 10 (ZT10) is peak REV-ERBα/β expression and these NRs can bind as a dimer to RORE repeats (DR2) and recruit the corepressor complex containing NCoR1/2 and HDAC3 thereby actively repressing transcription. At ZT22, REV-ERB expression is at its nadir, and ROR nuclear receptors bind to ROREs and recruit coactivators (CoAs) to induce transcription. Corepressors bound to REV-ERB at ZT10 are free to bind elsewhere and mediate transcription through other NRs, together or separately. Created with BioRender.

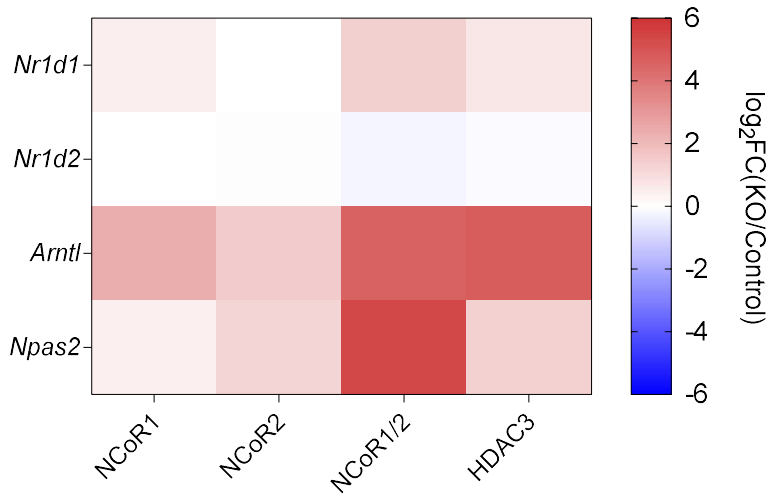

Figure 4.2. REV-ERB target gene expression in BAT corepressor KO models. Heat map of RNA-sequencing results from bulk brown adipose tissue from each corepressor KO (NCoR1, NCoR2, NCoR1/2-dKO, and HDAC3) displayed in log_2FC of the KO over Control expression. See methods of Chapter 2 for details.

BIBLIOGRAPHY

**Please note that Chapter 2 contains its own references section in publication format*

Adlanmerini, Marine, Bryce J. Carpenter, Jarrett R. Remsberg, Yann Aubert, Lindsey C. Peed, Hannah J. Richter, and Mitchell A. Lazar. 2019. “Circadian Lipid Synthesis in Brown Fat Maintains Murine Body Temperature during Chronic Cold.” *Proceedings of the National Academy of Sciences* 116 (37): 18691–99. https://doi.org/10.1073/pnas.1909883116.

Adlanmerini, Marine, Brianna M. Krusen, Hoang C. B. Nguyen, Clare W. Teng, Lauren N. Woodie, Michael C. Tackenberg, Caroline E. Geisler, et al. 2021. “REV-ERB Nuclear Receptors in the Suprachiasmatic Nucleus Control Circadian Period and Restrict Diet-Induced Obesity.” *Science Advances* 7 (44): eabh2007. https://doi.org/10.1126/sciadv.abh2007.

Adlanmerini, Marine, Hoang C. B. Nguyen, Brianna M. Krusen, Clare W. Teng, Caroline E. Geisler, Lindsey C. Peed, Bryce J. Carpenter, Matthew R. Hayes, and Mitchell A. Lazar. 2021. “Hypothalamic REV-ERB Nuclear Receptors Control Diurnal Food Intake and Leptin Sensitivity in Diet-Induced Obese Mice.” *The Journal of Clinical Investigation* 131 (1). https://doi.org/10.1172/JCI140424.

Aherne, W., and D. Hull. 1966. “Brown Adipose Tissue and Heat Production in the Newborn Infant.” *The Journal of Pathology and Bacteriology* 91 (1): 223–34. https://doi.org/10.1002/path.1700910126.

Albashir, Ahmed Abdalazim Dafallah. 2020. “The Potential Impacts of Obesity on COVID-19.” *Clinical Medicine* 20 (4): e109–13. https://doi.org/10.7861/clinmed.2020-0239.

Allada, Ravi, and Joseph Bass. 2021. “Circadian Mechanisms in Medicine.” *The New England Journal of Medicine* 384 (6): 550–61. https://doi.org/10.1056/NEJMra1802337.

Armingol, Erick, Adam Officer, Olivier Harismendy, and Nathan E. Lewis. 2021. “Deciphering Cell–Cell Interactions and Communication from Gene Expression.” *Nature Reviews Genetics* 22 (2): 71–88. https://doi.org/10.1038/s41576-020-00292-x.

Balsalobre, Aurélio, Francesca Damiola, and Ueli Schibler. 1998. “A Serum Shock Induces Circadian Gene Expression in Mammalian Tissue Culture Cells.” *Cell* 93 (6): 929–37. https://doi.org/10.1016/S0092-8674(00)81199-X.

Bartness, T. J., C. H. Vaughan, and C. K. Song. 2010. “Sympathetic and Sensory Innervation of Brown Adipose Tissue.” *International Journal of Obesity (2005)* 34 Suppl 1 (October): S36-42. https://doi.org/10.1038/ijo.2010.182.

Bass, Joseph. 2012. “Circadian Topology of Metabolism.” *Nature* 491 (7424): 348–56. https://doi.org/10.1038/nature11704.

Bolsoni-Lopes, Andressa, Yves Deshaies, and William T. Festuccia. 2015. “Regulation of Brown Adipose Tissue Recruitment, Metabolism and Thermogenic Function by Peroxisome Proliferator-Activated Receptor γ.” *Temperature (Austin, Tex.)* 2 (4): 476–82. https://doi.org/10.1080/23328940.2015.1011564.

Brück, Kurt. 1961. “Temperature Regulation in the Newborn Infant (Part 1 of 3).” *Neonatology* 3 (2–3): 65–81. https://doi.org/10.1159/000239810.

Bugge, Anne, Dan Feng, Logan J. Everett, Erika R. Briggs, Shannon E. Mullican, Fenfen Wang, Jennifer Jager, and Mitchell A. Lazar. 2012. “Rev-Erbα and Rev-Erbβ Coordinately Protect the Circadian Clock and Normal Metabolic Function.” *Genes & Development* 26 (7): 657–67. https://doi.org/10.1101/gad.186858.112.

Cannon, Barbara, and Jan Nedergaard. 2004. “Brown Adipose Tissue: Function and Physiological Significance.” *Physiological Reviews* 84 (1): 277–359. https://doi.org/10.1152/physrev.00015.2003.

Cawthorn, William P., and Jaswinder K. Sethi. 2008. “TNF-α and Adipocyte Biology.” *FEBS Letters* 582 (1): 117–31. https://doi.org/10.1016/j.febslet.2007.11.051.

Chandra, Vikas, Pengxiang Huang, Yoshitomo Hamuro, Srilatha Raghuram, Yongjun Wang, Thomas P. Burris, and Fraydoon Rastinejad. 2008. “Structure of the Intact PPAR-γ–RXR-α Nuclear Receptor Complex on DNA.” *Nature* 456 (7220): 350–56. https://doi.org/10.1038/nature07413.

Chitraju, Chandramohan, Alexander W. Fischer, Robert V. Farese, and Tobias C. Walther. 2020. “Lipid Droplets in Brown Adipose Tissue Are Dispensable for Cold-Induced Thermogenesis.” *Cell Reports* 33 (5): 108348. https://doi.org/10.1016/j.celrep.2020.108348.

Cho, Han, Xuan Zhao, Megumi Hatori, Ruth T. Yu, Grant D. Barish, Michael T. Lam, Ling-Wa Chong, et al. 2012. “Regulation of Circadian Behaviour and Metabolism by REV-ERB-α and REV-ERB-β.” *Nature* 485 (7396): 123–27. https://doi.org/10.1038/nature11048.

Claflin, Kristin E., Kyle H. Flippo, Andrew I. Sullivan, Meghan C. Naber, Bolu Zhou, Tate J. Neff, Sharon O. Jensen-Cody, and Matthew J. Potthoff. 2022. “Conditional Gene Targeting Using UCP1-Cre Mice Directly Targets the Central Nervous System beyond Thermogenic Adipose Tissues.” *Molecular Metabolism* 55 (January): 101405. https://doi.org/10.1016/j.molmet.2021.101405.

Chouchani, Edward T., Lawrence Kazak, and Bruce M. Spiegelman. 2019. “New Advances in Adaptive Thermogenesis: UCP1 and Beyond.” *Cell Metabolism* 29 (1): 27–37. https://doi.org/10.1016/j.cmet.2018.11.002.

Cypess, Aaron M., Sanaz Lehman, Gethin Williams, Ilan Tal, Dean Rodman, Allison B. Goldfine, Frank C. Kuo, et al. 2009. “Identification and Importance of Brown Adipose Tissue in Adult Humans.” *New England Journal of Medicine* 360 (15): 1509–17. https://doi.org/10.1056/NEJMoa0810780.

Cypess, Aaron M., Lauren S. Weiner, Carla Roberts-Toler, Elisa Franquet Elía, Skyler H. Kessler, Peter A. Kahn, Jeffrey English, et al. 2015. “Activation of Human Brown Adipose Tissue by a B3-Adrenergic Receptor Agonist.” *Cell Metabolism* 21 (1): 33–38. https://doi.org/10.1016/j.cmet.2014.12.009.

Dierickx, Pieterjan, Matthew J. Emmett, Chunjie Jiang, Kahealani Uehara, Manlu Liu, Marine Adlanmerini, and Mitchell A. Lazar. 2019. “SR9009 Has REV-ERB-Independent Effects on Cell Proliferation and Metabolism.” *Proceedings of the National Academy of Sciences of the United States of America* 116 (25): 12147–52. https://doi.org/10.1073/pnas.1904226116.

Dragano, Nathalia R. V., Johan Fernø, Carlos Diéguez, Miguel López, and Edward Milbank. 2020. “Recent Updates on Obesity Treatments: Available Drugs and Future Directions.” *Neuroscience* 437 (June): 215–39. https://doi.org/10.1016/j.neuroscience.2020.04.034.

Dumas, B, H P Harding, H S Choi, K A Lehmann, M Chung, M A Lazar, and D D Moore. 1994. “A New Orphan Member of the Nuclear Hormone Receptor Superfamily Closely Related to Rev-Erb.” *Molecular Endocrinology* 8 (8): 996–1005. https://doi.org/10.1210/mend.8.8.7997240.

Emmett, Matthew J., and Mitchell A. Lazar. 2019. “Integrative Regulation of Physiology by Histone Deacetylase 3.” *Nature Reviews. Molecular Cell Biology* 20 (2): 102–15. https://doi.org/10.1038/s41580-018-0076-0.

Emmett, Matthew J., Hee-Woong Lim, Jennifer Jager, Hannah J. Richter, Marine Adlanmerini, Lindsey C. Peed, Erika R. Briggs, et al. 2017. “Histone Deacetylase 3 Prepares Brown Adipose Tissue For Acute Thermogenic Challenge.” *Nature* 546 (7659): 544–48. https://doi.org/10.1038/nature22819.

Evans, Ronald M., and David J. Mangelsdorf. 2014. “Nuclear Receptors, RXR, and the Big Bang.” *Cell* 157 (1): 255–66. https://doi.org/10.1016/j.cell.2014.03.012.

Feng, Dan, Tao Liu, Zheng Sun, Anne Bugge, Shannon E. Mullican, Theresa Alenghat, X. Shirley Liu, and Mitchell A. Lazar. 2011. “A Circadian Rhythm Orchestrated by Histone Deacetylase 3 Controls Hepatic Lipid Metabolism.” *Science* 331 (6022): 1315–19. https://doi.org/10.1126/science.1198125.

Fischer, Katrin, Henry H. Ruiz, Kevin Jhun, Brian Finan, Douglas J. Oberlin, Verena van der Heide, Anastasia V. Kalinovich, et al. 2017. “Alternatively Activated Macrophages Do Not Synthesize Catecholamines or Contribute to Adipose Tissue Adaptive Thermogenesis.” *Nature Medicine* 23 (5): 623–30. https://doi.org/10.1038/nm.4316.

Forman, B M, J Chen, B Blumberg, S A Kliewer, R Henshaw, E S Ong, and R M Evans. 1994. “Cross-Talk among ROR Alpha 1 and the Rev-Erb Family of Orphan Nuclear Receptors.” *Molecular Endocrinology* 8 (9): 1253–61. https://doi.org/10.1210/mend.8.9.7838158.

Gerhart-Hines, Zachary, Dan Feng, Matthew J. Emmett, Logan J. Everett, Emanuele Loro, Erika R. Briggs, Anne Bugge, et al. 2013. “The Nuclear Receptor Rev-Erbα

Controls Circadian Thermogenic Plasticity." *Nature* 503 (7476): 410–13. https://doi.org/10.1038/nature12642.

Greenhill, Claire. 2021. "Role for IL-17A in Adipocyte Biology." *Nature Reviews Endocrinology* 17 (7): 383–383. https://doi.org/10.1038/s41574-021-00504-2.

Glass, Christopher K., and Michael G. Rosenfeld. 2000. "The Coregulator Exchange in Transcriptional Functions of Nuclear Receptors." *Genes & Development* 14 (2): 121–41. https://doi.org/10.1101/gad.14.2.121.

Guan, Dongyin, and Mitchell A. Lazar. 2021. "Interconnections between Circadian Clocks and Metabolism." *The Journal of Clinical Investigation* 131 (15). https://doi.org/10.1172/JCI148278.

Guan, Dongyin, Ying Xiong, Trang Minh Trinh, Yang Xiao, Wenxiang Hu, Chunjie Jiang, Pieterjan Dierickx, Cholsoon Jang, Joshua D. Rabinowitz, and Mitchell A. Lazar. 2020. "The Hepatocyte Clock and Feeding Control Chronophysiology of Multiple Liver Cell Types." *Science* 369 (6509): 1388–94. https://doi.org/10.1126/science.aba8984.

Guenther, Matthew G., Orr Barak, and Mitchell A. Lazar. 2001. "The SMRT and N-CoR Corepressors Are Activating Cofactors for Histone Deacetylase 3." *Molecular and Cellular Biology* 21 (18): 6091–6101. https://doi.org/10.1128/MCB.21.18.6091-6101.2001.

Hastings, Michael H., Elizabeth S. Maywood, and Marco Brancaccio. 2018. "Generation of Circadian Rhythms in the Suprachiasmatic Nucleus." *Nature Reviews Neuroscience* 19 (8): 453–69. https://doi.org/10.1038/s41583-018-0026-z.

Heaton, Gillian M., Rob J. Wagenvoord, Albertus KEMP Jr, and David G. Nicholls. 1978. "Brown-Adipose-Tissue Mitochondria: Photoaffinity Labelling of the Regulatory

Site of Energy Dissipation." *European Journal of Biochemistry* 82 (2): 515–21. https://doi.org/10.1111/j.1432-1033.1978.tb12045.x.

Heery, David M., Eric Kalkhoven, Susan Hoare, and Malcolm G. Parker. 1997. "A Signature Motif in Transcriptional Co-Activators Mediates Binding to Nuclear Receptors." *Nature* 387 (6634): 733–36. https://doi.org/10.1038/42750.

Henriksson, Emma, and Katja A. Lamia. 2015. "Adipose Clocks: Burning the Midnight Oil." *Journal of Biological Rhythms* 30 (5): 364–73. https://doi.org/10.1177/0748730415581234.

Hu, Bo, Chengcheng Jin, Xing Zeng, Jon M. Resch, Mark P. Jedrychowski, Zongfang Yang, Bhavna N. Desai, et al. 2020. "ΓδT Cells and Adipocyte IL-17RC Control Fat Innervation and Thermogenesis." *Nature* 578 (7796): 610–14. https://doi.org/10.1038/s41586-020-2028-z.

Hu, Xiao, Yun Li, and Mitchell A. Lazar. 2001. "Determinants of CoRNR-Dependent Repression Complex Assembly on Nuclear Hormone Receptors." *Molecular and Cellular Biology* 21 (5): 1747–58. https://doi.org/10.1128/MCB.21.5.1747-1758.2001.

Jeffery, Elise, Ryan Berry, Christopher D Church, Songtao Yu, Brett A Shook, Valerie Horsley, Evan D Rosen, and Matthew S Rodeheffer. 2014. "Characterization of Cre Recombinase Models for the Study of Adipose Tissue." *Adipocyte* 3 (3): 206–11. https://doi.org/10.4161/adip.29674.

Jepsen, Kristen, Ola Hermanson, Thandi M Onami, Anatoli S Gleiberman, Victoria Lunyak, Robert J McEvilly, Riki Kurokawa, et al. 2000. "Combinatorial Roles of the Nuclear Receptor Corepressor in Transcription and Development." *Cell* 102 (6): 753–63. https://doi.org/10.1016/S0092-8674(00)00064-7.

Jepsen, Kristen, Derek Solum, Tianyuan Zhou, Robert J. McEvilly, Hyun-Jung Kim, Christopher K. Glass, Ola Hermanson, and Michael G. Rosenfeld. 2007. “SMRT-Mediated Repression of an H3K27 Demethylase in Progression from Neural Stem Cell to Neuron.” *Nature* 450 (7168): 415–19. https://doi.org/10.1038/nature06270.

Kim, Yong Hoon, Sajid A. Marhon, Yuxiang Zhang, David J. Steger, Kyoung-Jae Won, and Mitchell A. Lazar. 2018. “Rev-Erbα Dynamically Modulates Chromatin Looping to Control Circadian Gene Transcription.” *Science (New York, N.Y.)* 359 (6381): 1274–77. https://doi.org/10.1126/science.aao6891.

Kohlgruber, Ayano C., Shani T. Gal-Oz, Nelson M. LaMarche, Moto Shimazaki, Danielle Duquette, Hui-Fern Koay, Hung N. Nguyen, et al. 2018. “Γδ T Cells Producing Interleukin-17A Regulate Adipose Regulatory T Cell Homeostasis and Thermogenesis.” *Nature Immunology* 19 (5): 464–74. https://doi.org/10.1038/s41590-018-0094-2.

Kroon, Jan, Maaike Schilperoort, Wietse In Het Panhuis, Rosa van den Berg, Lotte van Doeselaar, Cristy R. C. Verzijl, Nikki van Trigt, et al. 2021. “A Physiological Glucocorticoid Rhythm Is an Important Regulator of Brown Adipose Tissue Function.” *Molecular Metabolism* 47 (May): 101179. https://doi.org/10.1016/j.molmet.2021.101179.

Kujirai, Tomoya, and Hitoshi Kurumizaka. 2020. “Transcription through the Nucleosome.” *Current Opinion in Structural Biology*, Theory and Simulation ● Macromolecular Assemblies, 61 (April): 42–49. https://doi.org/10.1016/j.sbi.2019.10.007.

Lazar, M A, R A Hodin, D S Darling, and W W Chin. 1989. “A Novel Member of the Thyroid/Steroid Hormone Receptor Family Is Encoded by the Opposite Strand of

the Rat c-ErbA Alpha Transcriptional Unit." *Molecular and Cellular Biology* 9 (3): 1128–36.

Li, Pingping, Wuqiang Fan, Jianfeng Xu, Min Lu, Hiroyasu Yamamoto, Johan Auwerx, Dorothy D. Sears, et al. 2011. "Adipocyte NCoR Knockout Decreases PPARγ Phosphorylation and Enhances PPARγ Activity and Insulin Sensitivity." *Cell* 147 (4): 815–26. https://doi.org/10.1016/j.cell.2011.09.050.

Li, Pingping, Nathanael J. Spann, Minna U. Kaikkonen, Min Lu, Da Young Oh, Jesse N. Fox, Gautam Bandyopadhyay, et al. 2013. "NCoR Repression of LXRs Restricts Macrophage Biosynthesis of Insulin-Sensitizing Omega 3 Fatty Acids." *Cell* 155 (1): 200–214. https://doi.org/10.1016/j.cell.2013.08.054.

Lidell, Martin E. 2019. "Brown Adipose Tissue in Human Infants." In *Brown Adipose Tissue*, edited by Alexander Pfeifer, Martin Klingenspor, and Stephan Herzig, 107–23. *Handbook of Experimental Pharmacology.* Cham: Springer International Publishing. https://doi.org/10.1007/164_2018_118.

Lombardi, Patrick M, Kathryn E Cole, Daniel P Dowling, and David W Christianson. 2011. "Structure, Mechanism, and Inhibition of Histone Deacetylases and Related Metalloenzymes." *Current Opinion in Structural Biology, Proteins/Catalysis and regulation*, 21 (6): 735–43. https://doi.org/10.1016/j.sbi.2011.08.004.

Lumeng, Carey N., and Alan R. Saltiel. 2011. "Inflammatory Links between Obesity and Metabolic Disease." *The Journal of Clinical Investigation* 121 (6): 2111–17. https://doi.org/10.1172/JCI57132.

Marken Lichtenbelt, Wouter D. van, Joost W. Vanhommerig, Nanda M. Smulders, Jamie M.A.F.L. Drossaerts, Gerrit J. Kemerink, Nicole D. Bouvy, Patrick Schrauwen, and G.J. Jaap Teule. 2009. "Cold-Activated Brown Adipose Tissue in Healthy

Men.” *New England Journal of Medicine* 360 (15): 1500–1508. https://doi.org/10.1056/NEJMoa0808718.

Meister, Benjamin M., Soon-Gook Hong, Junchul Shin, Meghan Rath, Jacqueline Sayoc, and Joon-Young Park. 2022. “Healthy versus Unhealthy Adipose Tissue Expansion: The Role of Exercise.” *Journal of Obesity & Metabolic Syndrome* 31 (1): 37–50. https://doi.org/10.7570/jomes21096.

Mrzilkova, J., P. Michenka, M. Seremeta, J. Kremen, J. Dudak, J. Zemlicka, V. Musil, B. Minnich, and P. Zach. 2020. “Morphology of the Vasculature and Blood Supply of the Brown Adipose Tissue Examined in an Animal Model by Micro-CT.” *BioMed Research International* 2020: 7502578. https://doi.org/10.1155/2020/7502578.

Mullican, Shannon E., Takuya Tomaru, Christine A. Gaddis, Lindsey C. Peed, Anand Sundaram, and Mitchell A. Lazar. 2013. “A Novel Adipose-Specific Gene Deletion Model Demonstrates Potential Pitfalls of Existing Methods.” *Molecular Endocrinology* 27 (1): 127–34. https://doi.org/10.1210/me.2012-1267.

Nagy, Laszlo, Hung-Ying Kao, James D. Love, Chuan Li, Ester Banayo, John T. Gooch, V. Krishna, K. Chatterjee, Ronald M. Evans, and John W.R. Schwabe. 1999. “Mechanism of Corepressor Binding and Release from Nuclear Hormone Receptors.” *Genes & Development* 13 (24): 3209–16.

Nagy, Laszlo, and John W. R. Schwabe. 2004. “Mechanism of the Nuclear Receptor Molecular Switch.” *Trends in Biochemical Sciences* 29 (6): 317–24. https://doi.org/10.1016/j.tibs.2004.04.006.

Nedergaard, Jan, Barbara Cannon, and Olov Lindberg. 1977. “Microcalorimetry of Isolated Mammalian Cells.” *Nature* 267 (5611): 518–20. https://doi.org/10.1038/267518a0.

Nedergaard, Jan, and Olov Lindberg. 1979. “Norepinephrine-Stimulated Fatty-Acid Release and Oxygen Consumption in Isolated Hamster Brown-Fat Cells.” *European Journal of Biochemistry* 95 (1): 139–45. https://doi.org/10.1111/j.1432-1033.1979.tb12948.x.

Nguyen, Khoa D., Yifu Qiu, Xiaojin Cui, Y.P. Sharon Goh, Julia Mwangi, Tovo David, Lata Mukundan, Frank Brombacher, Richard M. Locksley, and Ajay Chawla. 2011. “Alternatively Activated Macrophages Produce Catecholamines to Sustain Adaptive Thermogenesis.” *Nature* 480 (7375): 104–8. https://doi.org/10.1038/nature10653.

Nicholls, D. G., and R. M. Locke. 1984. “Thermogenic Mechanisms in Brown Fat.” *Physiological Reviews* 64 (1): 1–64. https://doi.org/10.1152/physrev.1984.64.1.1.

Nofsinger, Russell R., Pingping Li, Suk-Hyun Hong, Johan W. Jonker, Grant D. Barish, Hao Ying, Sheue-yann Cheng, et al. 2008. “SMRT Repression of Nuclear Receptors Controls the Adipogenic Set Point and Metabolic Homeostasis.” *Proceedings of the National Academy of Sciences of the United States of America* 105 (50): 20021–26. https://doi.org/10.1073/pnas.0811012105.

Partch, Carrie L., Carla B. Green, and Joseph S. Takahashi. 2014. “Molecular Architecture of the Mammalian Circadian Clock.” *Trends in Cell Biology* 24 (2): 90–99. https://doi.org/10.1016/j.tcb.2013.07.002.

Pei, Liming, Mathias Leblanc, Grant Barish, Annette Atkins, Russell Nofsinger, Jamie Whyte, David Gold, et al. 2011. “Thyroid Hormone Receptor Repression Is Linked to Type I Pneumocyte–Associated Respiratory Distress Syndrome.” *Nature Medicine* 17 (11): 1466–72. https://doi.org/10.1038/nm.2450.

Pestel, Julien, Marwa Chehimi, Mélanie Bonhomme, Maud Robert, Hubert Vidal, and Assia Eljaafari. 2020. “IL-17A Contributes to Propagation of Inflammation but Does Not Impair Adipogenesis and/or Insulin Response, in Adipose Tissue of Obese Individuals.” *Cytokine* 126 (February): 154865. https://doi.org/10.1016/j.cyto.2019.154865.

Privalsky, Martin L. 2004. “The Role of Corepressors in Transcriptional Regulation by Nuclear Hormone Receptors.” *Annual Review of Physiology* 66: 315–60. https://doi.org/10.1146/annurev.physiol.66.032802.155556.

Rasmussen, A. T. 1923. “The So-Called Hibernating Gland.” *Journal of Morphology* 38 (1): 147–205. https://doi.org/10.1002/jmor.1050380106.

Reilly, Shannon M., Prerna Bhargava, Sihao Liu, Matthew R. Gangl, Cem Gorgun, Russell R. Nofsinger, Ronald M. Evans, Lu Qi, Frank B. Hu, and Chih-Hao Lee. 2010. “Nuclear Receptor Co-Repressor SMRT Regulates Mitochondrial Oxidative Metabolism and Mediates Aging Related Metabolic Deterioration.” *Cell Metabolism* 12 (6): 643–53. https://doi.org/10.1016/j.cmet.2010.11.007.

Retnakaran, R, G Flock, and V Giguère. 1994. “Identification of RVR, a Novel Orphan Nuclear Receptor That Acts as a Negative Transcriptional Regulator.” *Molecular Endocrinology* 8 (9): 1234–44. https://doi.org/10.1210/mend.8.9.7838156.

Reyes, Alexis A., Ryan D. Marcum, and Yuan He. 2021. “Structure and Function of Chromatin Remodelers.” *Journal of Molecular Biology* 433 (14): 166929. https://doi.org/10.1016/j.jmb.2021.166929.

Ricquier, Daniel, and Jean-Claude Kader. 1976. “Mitochondrial Protein Alteration in Active Brown Fat: A Sodium Dodecyl Sulfate-Polyacrylamide Gel Electrophoretic Study.” *Biochemical and Biophysical Research Communications* 73 (3): 577–83. https://doi.org/10.1016/0006-291X(76)90849-4.

Ritter, Megan J., Izuki Amano, Norihiro Imai, Lorraine Soares De Oliveira, Kristen R. Vella, and Anthony N. Hollenberg. 2021. “Nuclear Receptor CoRepressors, NCOR1 and SMRT, Are Required for Maintaining Systemic Metabolic Homeostasis.” *Molecular Metabolism* 53 (November): 101315. https://doi.org/10.1016/j.molmet.2021.101315.

Roesler, Anna, and Lawrence Kazak. 2020. “UCP1-Independent Thermogenesis.” *Biochemical Journal* 477 (3): 709–25. https://doi.org/10.1042/BCJ20190463.

Romanelli, Steven M., Kenneth T. Lewis, Akira Nishii, Alan C. Rupp, Ziru Li, Hiroyuki Mori, Rebecca L. Schill, Brian S. Learman, Christopher J. Rhodes, and Ormond A. MacDougald. 2021. “BAd-CRISPR: Inducible Gene Knockout in Interscapular Brown Adipose Tissue of Adult Mice.” *Journal of Biological Chemistry* 297 (6). https://doi.org/10.1016/j.jbc.2021.101402.

Ruban, Aruchuna, Kostadin Stoenchev, Hutan Ashrafian, and Julian Teare. 2019. “Current Treatments for Obesity.” *Clinical Medicine* 19 (3): 205–12. https://doi.org/10.7861/clinmedicine.19-3-205.

Schäffler, Andreas, and Jürgen Schölmerich. 2010. “Innate Immunity and Adipose Tissue Biology.” *Trends in Immunology* 31 (6): 228–35. https://doi.org/10.1016/j.it.2010.03.001.

Schmidt, Søren Fisker, Bjørk Ditlev Larsen, Anne Loft, and Susanne Mandrup. 2016. “Cofactor Squelching: Artifact or Fact?” *BioEssays: News and Reviews in Molecular, Cellular and Developmental Biology* 38 (7): 618–26. https://doi.org/10.1002/bies.201600034.

Schreiber, Renate, Clemens Diwoky, Gabriele Schoiswohl, Ursula Feiler, Nuttaporn Wongsiriroj, Mahmoud Abdellatif, Dagmar Kolb, et al. 2017. “Cold-Induced Thermogenesis Depends on ATGL-Mediated Lipolysis in Cardiac Muscle, but

Not Brown Adipose Tissue." *Cell Metabolism* 26 (5): 753-763.e7. https://doi.org/10.1016/j.cmet.2017.09.004.

Shabtai, Yehuda, Nagaswaroop K. Nagaraj, Kirill Batmanov, Young-Wook Cho, Yuxia Guan, Chunjie Jiang, Jarrett Remsberg, Douglas Forrest, and Mitchell A. Lazar. 2021. "A Coregulator Shift, Rather than the Canonical Switch, Underlies Thyroid Hormone Action in the Liver." *Genes & Development* 35 (5–6): 367–78. https://doi.org/10.1101/gad.345686.120.

Sheldon, Elroy F. 1924. "The So-Called Hibernating Gland in Mammals: A Form of Adipose Tissue." *The Anatomical Record* 28 (5): 331–47. https://doi.org/10.1002/ar.1090280502.

Shin, Hyunsu, Yinyan Ma, Tatyana Chanturiya, Qiang Cao, Youlin Wang, Anil K. G. Kadegowda, Rachel Jackson, et al. 2017. "Lipolysis in Brown Adipocytes Is Not Essential for Cold-Induced Thermogenesis in Mice." *Cell Metabolism* 26 (5): 764-777.e5. https://doi.org/10.1016/j.cmet.2017.09.002.

Sideli, Lucia, Gianluca Lo Coco, Rubinia Celeste Bonfanti, Bianca Borsarini, Lucia Fortunato, Cristina Sechi, and Nadia Micali. 2021. "Effects of COVID-19 Lockdown on Eating Disorders and Obesity: A Systematic Review and Meta-Analysis." *European Eating Disorders Review: The Journal of the Eating Disorders Association* 29 (6): 826–41. https://doi.org/10.1002/erv.2861.

Solt, Laura A, Douglas J Kojetin, and Thomas P Burris. 2011. "The REV-ERBs and RORs: Molecular Links between Circadian Rhythms and Lipid Homeostasis." *Future Medicinal Chemistry* 3 (5): 623–38. https://doi.org/10.4155/fmc.11.9.

Sostre-Colón, Jaimarie, Kahealani Uehara, Anna E. Garcia Whitlock, Matthew J. Gavin, Jeff Ishibashi, Matthew J. Potthoff, Patrick Seale, and Paul M. Titchenell. 2021. "Hepatic AKT Orchestrates Adipose Tissue Thermogenesis via FGF21-

Dependent and -Independent Mechanisms." *Cell Reports* 35 (7): 109128. https://doi.org/10.1016/j.celrep.2021.109128.

Strahl, Brian D., and C. David Allis. 2000. "The Language of Covalent Histone Modifications." *Nature* 403 (6765): 41–45. https://doi.org/10.1038/47412.

Sun, Kai, Christine M. Kusminski, and Philipp E. Scherer. 2011. "Adipose Tissue Remodeling and Obesity." *The Journal of Clinical Investigation* 121 (6): 2094–2101. https://doi.org/10.1172/JCI45887.

Sun, Wenfei, Hua Dong, Miroslav Balaz, Michal Slyper, Eugene Drokhlyansky, Georgia Colleluori, Antonio Giordano, et al. 2020. "SnRNA-Seq Reveals a Subpopulation of Adipocytes That Regulates Thermogenesis." *Nature* 587 (7832): 98–102. https://doi.org/10.1038/s41586-020-2856-x.

Sun, Zheng, Dan Feng, Bin Fang, Shannon E. Mullican, Seo-Hee You, Hee-Woong Lim, Logan J. Everett, et al. 2013. "Deacetylase-Independent Function of HDAC3 in Transcription and Metabolism Requires Nuclear Receptor Corepressor." *Molecular Cell* 52 (6): 769–82. https://doi.org/10.1016/j.molcel.2013.10.022.

Sutanto, Maria M., Kelly K. Ferguson, Hiroya Sakuma, Honggang Ye, Matthew J. Brady, and Ronald N. Cohen. 2010. "The Silencing Mediator of Retinoid and Thyroid Hormone Receptors (SMRT) Regulates Adipose Tissue Accumulation and Adipocyte Insulin Sensitivity in Vivo." *The Journal of Biological Chemistry* 285 (24): 18485–95. https://doi.org/10.1074/jbc.M110.107680.

Szigety, Katherine M., Fang Liu, Chase Y. Yuan, Deborah J. Moran, Jeremy Horrell, Heather R. Gochnauer, Ronald N. Cohen, et al. 2020. "HDAC3 Ensures Stepwise Epidermal Stratification via NCoR/SMRT-Reliant Mechanisms Independent of Its Histone Deacetylase Activity." *Genes & Development* 34 (13–14): 973–88. https://doi.org/10.1101/gad.333674.119.

Tabuchi, Chihiro, and Hei Sook Sul. 2021. “Signaling Pathways Regulating Thermogenesis.” *Frontiers in Endocrinology* 12. https://www.frontiersin.org/article/10.3389/fendo.2021.595020.

Tackenberg, Michael C., Jeff R. Jones, Terry L. Page, and Jacob J. Hughey. 2018. “Tau-Independent Phase Analysis: A Novel Method for Accurately Determining Phase Shifts.” *Journal of Biological Rhythms* 33 (3): 223–32. https://doi.org/10.1177/0748730418768116.

Takahashi, Joseph S., Hee-Kyung Hong, Caroline H. Ko, and Erin L. McDearmon. 2008. “The Genetics of Mammalian Circadian Order and Disorder: Implications for Physiology and Disease.” *Nature Reviews Genetics* 9 (10): 764–75. https://doi.org/10.1038/nrg2430.

Teijeiro, Ana, Amanda Garrido, Anna Ferre, Cristian Perna, and Nabil Djouder. 2021. “Inhibition of the IL-17A Axis in Adipocytes Suppresses Diet-Induced Obesity and Metabolic Disorders in Mice.” *Nature Metabolism* 3 (4): 496–512. https://doi.org/10.1038/s42255-021-00371-1.

Tolsma, Thomas O., and Jeffrey C. Hansen. 2019. “Post-Translational Modifications and Chromatin Dynamics.” *Essays in Biochemistry* 63 (1): 89–96. https://doi.org/10.1042/EBC20180067.

Tsai, V. W. W., S. Lin, D. A. Brown, A. Salis, and S. N. Breit. 2016. “Anorexia-Cachexia and Obesity Treatment May Be Two Sides of the Same Coin: Role of the TGF-b Superfamily Cytokine MIC-1/GDF15.” *International Journal of Obesity (2005)* 40 (2): 193–97. https://doi.org/10.1038/ijo.2015.242.

Ukropec, Jozef, Rea P. Anunciado, Yann Ravussin, Matthew W. Hulver, and Leslie P. Kozak. 2006. “UCP1-Independent Thermogenesis in White Adipose Tissue of

Cold-Acclimated Ucp1-/- Mice *." *Journal of Biological Chemistry* 281 (42): 31894–908. https://doi.org/10.1016/S0021-9258(19)84104-2.

Van Hauwaert, Elvira Laila, Ellen Gammelmark, Anitta Kinga Sárvári, Lena Larsen, Ronni Nielsen, Jesper Grud Skat Madsen, and Susanne Mandrup. 2021. "Isolation of Nuclei from Mouse White Adipose Tissues for Single-Nucleus Genomics." *STAR Protocols* 2 (3): 100612. https://doi.org/10.1016/j.xpro.2021.100612.

Vieira, Cristiano Pedrozo, Leticia Prado de Oliveira, Mariana Bombardi Da Silva, Diana Majolli Andre, Edith Bastos Gandra Tavares, Edson Rosa Pimentel, and Edson Antunes. 2020. "Role of Metalloproteinases and TNF-α in Obesity-Associated Asthma in Mice." *Life Sciences* 259 (October): 118191. https://doi.org/10.1016/j.lfs.2020.118191.

Vieira, Elaine, Elena G. Ruano, Ana Lucia C. Figueroa, Gloria Aranda, Dulce Momblan, Francesc Carmona, Ramon Gomis, Josep Vidal, and Felicia A. Hanzu. 2014. "Altered Clock Gene Expression in Obese Visceral Adipose Tissue Is Associated with Metabolic Syndrome." *PLOS ONE* 9 (11): e111678. https://doi.org/10.1371/journal.pone.0111678.

Vishvanath, Lavanya, and Rana K. Gupta. 2019. "Contribution of Adipogenesis to Healthy Adipose Tissue Expansion in Obesity." *The Journal of Clinical Investigation* 129 (10): 4022–31. https://doi.org/10.1172/JCI129191.

Wang, Wenshan, and Patrick Seale. 2016. "Control of Brown and Beige Fat Development." *Nature Reviews. Molecular Cell Biology* 17 (11): 691–702. https://doi.org/10.1038/nrm.2016.96.

Wang, Youfa, May A Beydoun, Jungwon Min, Hong Xue, Leonard A Kaminsky, and Lawrence J Cheskin. 2020. "Has the Prevalence of Overweight, Obesity and

Central Obesity Levelled off in the United States? Trends, Patterns, Disparities, and Future Projections for the Obesity Epidemic." *International Journal of Epidemiology* 49 (3): 810–23. https://doi.org/10.1093/ije/dyz273.

Watson, Peter J., Louise Fairall, Guilherme M. Santos, and John W. R. Schwabe. 2012. "Structure of HDAC3 Bound to Co-Repressor and Inositol Tetraphosphate." *Nature* 481 (7381): 335–40. https://doi.org/10.1038/nature10728.

Weikum, Emily R., Xu Liu, and Eric A. Ortlund. 2018. "The Nuclear Receptor Superfamily: A Structural Perspective." *Protein Science: A Publication of the Protein Society* 27 (11): 1876–92. https://doi.org/10.1002/pro.3496.

Yamamoto, Hiroyasu, Evan G. Williams, Laurent Mouchiroud, Carles Canto, Weiwei Fan, Michael Downes, Christophe Héligon, et al. 2011. "NCoR1 Is a Conserved Physiological Modulator of Muscle Mass and Oxidative Function." *Cell* 147 (4): 827–39. https://doi.org/10.1016/j.cell.2011.10.017.

Yang, Xiaoyong, and Hai-Bin Ruan. 2015. "Neuronal Control of Adaptive Thermogenesis." *Frontiers in Endocrinology* 6 (September): 149. https://doi.org/10.3389/fendo.2015.00149.

Yin, Lei, and Mitchell A. Lazar. 2005. "The Orphan Nuclear Receptor Rev-Erbα Recruits the N-CoR/Histone Deacetylase 3 Corepressor to Regulate the Circadian Bmal1 Gene." *Molecular Endocrinology* 19 (6): 1452–59. https://doi.org/10.1210/me.2005-0057.

You, Seo-Hee, Hee-Woong Lim, Zheng Sun, Molly Broache, Kyoung-Jae Won, and Mitchell A. Lazar. 2013. "Nuclear Receptor Co-Repressors Are Required for the Histone-Deacetylase Activity of HDAC3 in Vivo." *Nature Structural & Molecular Biology* 20 (2): 182–87. https://doi.org/10.1038/nsmb.2476.

Zhang, Yuxiang, Bin Fang, Matthew J. Emmett, Manashree Damle, Zheng Sun, Dan Feng, Sean M. Armour, et al. 2015. “Discrete Functions of Nuclear Receptor Rev-Erbα Couple Metabolism to the Clock.” *Science (New York, N.Y.)* 348 (6242): 1488–92. https://doi.org/10.1126/science.aab3021.